

# On the Characterization of Dynamic Supramolecular Systems: A General Mathematical Association Model for Linear Supramolecular Copolymers and Application on a Complex Two-Component Hydrogen-Bonding System

Fabrice G. J. Odille,<sup>[a]</sup> Stefán Jónsson,<sup>[a]</sup> Susann Stjernqvist,<sup>[b]</sup> Tobias Rydén,<sup>\*,[b]</sup> and Kenneth Wärnmark<sup>\*,[a]</sup>

**Abstract:** A general mathematical model for the characterization of the dynamic (kinetically labile) association of supramolecular assemblies in solution is presented. It is an extension of the equal  $K$  (EK) model by the stringent use of linear algebra to allow for the simultaneous presence of an unlimited number of different units in the resulting assemblies. It allows for the analysis of highly complex dynamic equilibrium systems in solution, including both supramolecular homo- and copolymers without the recourse to extensive approximations, in a field in which other analytical methods are difficult. The derived mathematical methodology makes it possible to analyze dynamic systems such as supramolecular copolymers regarding for instance

the degree of polymerization, the distribution of a given monomer in different copolymers as well as its position in an aggregate. It is to date the only general means to characterize weak supramolecular systems. The model was fitted to NMR dilution titration data by using the program Matlab<sup>®</sup>, and a detailed algorithm for the optimization of the different parameters has been developed. The methodology is applied to a case study, a hydrogen-bonded supramolecular system, salen 4+porphyrin 5. The system is formally

a two-component system but in reality a three-component system. This results in a complex dynamic system in which all monomers are associated to each other by hydrogen bonding with different association constants, resulting in homo- and copolymers 4,5<sub>m</sub> as well as cyclic structures 6 and 7, in addition to free 4 and 5. The system was analyzed by extensive NMR dilution titrations at variable temperatures. All chemical shifts observed at different temperatures were used in the fitting to obtain the  $\Delta H^\circ$  and  $\Delta S^\circ$  values producing the best global fit. From the derived general mathematical expressions, system 4+5 could be characterized with respect to above-mentioned parameters.


**Keywords:** analytical methods • mathematical chemistry • NMR spectroscopy • polymers • supramolecular chemistry

## Introduction

One of the inherent challenges in the study of self-assembling processes in solution is the characterization of the chemically different assemblies that constitute the equilibrium mixture. In many cases the interactions between the components constituting each assembly are strong and/or kinetically inert and the number of chemically different assemblies is limited so that techniques like NMR spectroscopy, electrospray ionization mass spectrometry (ESIMS), size exclusion chromatography (SEC), viscometry, vapor pressure osmometry (VPO), and analytical ultracentrifugation (AU) can be used in the elucidation of the composition and/or structure.<sup>[1]</sup> In contrast there are many cases in which the species exist in low concentration, or in which the interactions between the different components are weak and/or ki-

[a] Dr. F. G. J. Odille, Dr. S. Jónsson, Dr. K. Wärnmark  
Organic Chemistry, Department of Chemistry  
Lund University, P.O. Box 124, 221 00 Lund (Sweden)  
Fax: (+46) 46-222-8209  
E-mail: Kenneth.Warnmark@organic.lu.se

[b] S. Stjernqvist, Prof. T. Rydén  
Centre for Mathematical Sciences  
Lund University, P.O. Box 118, 221 00 Lund (Sweden)  
Fax: (+46) 46-222-4623  
E-mail: Tobias.Ryden@matstat.lu.se

 Supporting information for this article is available on the WWW under <http://www.chemeurj.org/> or from the author. It contains a detailed description of the algorithm of the fitting of the model to the NMR dilution titration data as well as a description of the titrations and tables containing the primary data from the dilution titrations.

netically labile, making the composition of the system concentration-dependent. In such cases, the different assemblies formed upon aggregation cannot be characterized by the techniques mentioned above, and in practice, a rigorous mathematical treatment of association models will be the sole means to acquire information about the composition and association constants of the different possible assemblies.

In the case of supramolecular polymers, the analysis of the composition is particularly important. Assembly of monomers containing two or more binding sites occurs by noncovalent bonds such as hydrogen bonds,  $\pi$ - $\pi$  interactions, or metal coordination, resulting in linear or branched assemblies, dendrimers, or liquid crystals.<sup>[2]</sup> In the past decade, the interest in such polymers has grown considerably in attempts to obtain polymeric materials with new properties compared to covalent polymers.<sup>[2h]</sup> Moreover, supramolecular polymers formed by hydrogen bonding between monomers have been popular ever since the appearance of the field.<sup>[3,4]</sup> More specifically, in the quest for polymers with new properties, hydrogen-bonded supramolecular copolymers are attractive because of the ability of easily adjusting the property of a given polymer by simply adding another type of monomer to the solution.<sup>[5]</sup> Due to the relatively low barriers of activation involved in bond-breaking and bond-formation of hydrogen bonds, hydrogen-bonded supramolecular polymers will immediately respond to external stimuli. For instance, new copolymers are formed by addition of another type of monomer and rearrangement to form the most stable association of monomers.

One important objective in the field is to correlate the properties of the supramolecular copolymers with their compositions. So far only copolymers containing two different monomers have been assembled and most of the reported copolymers are alternating copolymers, ...ABABAB... In general, these are obtained by using one monomer, A, with the same hydrogen-bonding motif in its two ends, and another monomer, B, with a different, but complementary motif to A, in its two ends. The reason why supramolecular copolymers that do not contain more than two different types of monomers or supramolecular polymers of two monomers with different topology than the ones above have not been used, might be the difficulties in their characterization. Due to the fact that many hydrogen-bonded supramolecular polymers constitute rapid equilibrium systems, their composition will be concentration-dependent. This makes the use of classical polymer techniques of little applicability already for systems with only one monomer,<sup>[4a,6]</sup> and it is virtually impossible to characterize systems of more than one type of monomer, supramolecular copolymers, in which many more equilibria with different association constants are involved.<sup>[5b]</sup> Recently, promising techniques have been introduced to characterize supramolecular oligomers and polymers.

1) Chain stoppers have been introduced at the ends of the polymers to block the concentration dependence of the molecular mass of the aggregates.<sup>[6]</sup>

- 2) The presence of cyclic dimers in mixtures of supramolecular polymers have been detected by comparing diffusion coefficients, and thereby masses,<sup>[7d,e]</sup> obtained by pulsed-field-gradient (PFG) NMR techniques such as diffusion-ordered spectroscopy (DOSY).<sup>[7]</sup>
- 3) Identification of next neighbors in supramolecular copolymers have been achieved by fluorescence spectroscopy of labeled monomers.<sup>[8]</sup>
- 4) Very recently a supramolecular oligomer of a defined length was assembled using the principle of Vernier assemblies.<sup>[9]</sup>

In contrast, for dynamic (generally weakly associated) multi-component supramolecular systems the techniques 1) and 3) are difficult to employ.<sup>[10]</sup> The same is true for method 2).<sup>[11]</sup> In method 4) multiple binding-sites are needed and has so far been applied only to systems containing relatively strong binding sites.

In contrast, the characterization of dynamic supramolecular copolymers by NMR dilution titrations<sup>[12]</sup> to fit equilibrium models to observed changes in chemical shift of average proton resonances with concentration has not yet been fully recognized. So far, the NMR titration characterization of one polymeric system consisting of two different aromatic molecules, aggregating by  $\pi$ -stacking has been reported,<sup>[13]</sup> and analyses of supramolecular copolymers have been performed by using the dimerization model,<sup>[14]</sup> instead of a general association model.

We have developed a general approach to characterize dynamic supramolecular polymers by the application of an advanced mathematical treatment based on a general association model. It allows for the characterization of supramolecular copolymers in terms of speciation in solution, and for determination of the location of a particular monomer in a given assembly. A less general mathematical approach has been reported earlier by Veselkov.<sup>[13]</sup> Although the mathematical derivation of the expressions for the characterization of supramolecular copolymers is strictly done for linear aggregates, the present model is also extended to include cyclic structures as demonstrated in the case study (vide infra). The model is general for dynamic (kinetically labile) multicomponent systems with two binding sites, and it is independent of the technique used to extract equilibrium data. Here it will be applied to NMR dilution titrations. The most important feature of this treatment is that it allows for the extraction of information from spectroscopic data regarding the characterization of weak supramolecular assemblies. For such systems, the characterization is almost impossible by other means. The present methodology seems to be the only general one to date.

The association constants are key parameters in the characterization of supramolecular copolymers. For supramolecular hydrogen-bonded copolymers the association constants between the monomers are often estimated from the association constant of the monofunctionalized analogue of the monomers, resulting in dimerization constants instead of true association constants.<sup>[14]</sup> Linear aggregation of two dif-

ferent monomers have been described by the use of isodesmic models (vide infra).<sup>[15]</sup> However, there are limitations in their application or theoretical approach.<sup>[16]</sup> Another approach is more general, but the derivations are made in ways that do not generalize to systems higher than those containing two different monomers.<sup>[13]</sup> For supramolecular copolymers with more than two monomers and different self-association constants, the recognition motif of each of the monomers has not been programmed to form predominantly one type of association, and accordingly to date, there is no reported method to derive the association constants for such complicated systems. Therefore, the so-produced copolymers cannot be fully characterized.

Our approach to the problem of characterizing dynamic supramolecular systems stems from our interest in the field of less-rigid artificial-enzyme models,<sup>[17]</sup> in which we recently designed a catalytic supramolecular system in which all recognition motifs, both between catalyst subunits and between substrate and catalyst, are kinetically labile.<sup>[18]</sup> The system was designed to have a catalytic cavity **1** composed of a manganese–salen complex **2** as the catalyst and a zinc–porphyrin **3** as the receptor (Figure 1). The ultimate aim of the

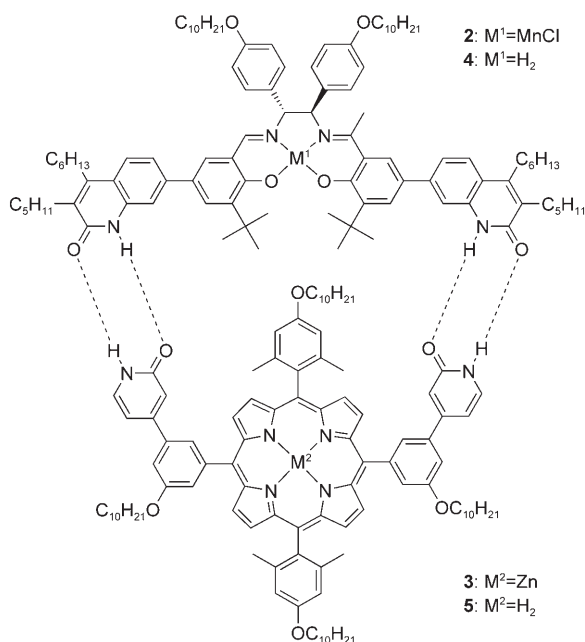


Figure 1. Representation of system **1** (**2**+**3**) and metal-free **6** (**4**+**5**).

design of macrocycle **1** is to catalyze the epoxidation of pyridyl appended olefins at the expense of phenyl appended ones. The catalyst and the receptor parts interact by two 2-pyridone self-complementary hydrogen-bonding motifs attached to each component. The binary hydrogen-bonding system of type acceptor–donor (AD) of the 2-pyridone motif was chosen to ensure a kinetically labile system,<sup>[19]</sup> and the pre-organization of the two 2-pyridone motifs of

each of **2** and **3** was designed to give rise to an AD//DA–DA//AD motif in **1**.<sup>[20]</sup>

Since it is entropically more favorable to form discrete cyclic species than polymers, macrocycle **1** was thought to be the major species in the solution at the concentration for the catalytic reaction. This hypothesis was used in our preliminary study.<sup>[18a]</sup> Indeed, in the epoxidations, the system **2**+**3** exhibited higher selectivity for pyridine-appended styrenes than the phenyl ones (Figure 2).<sup>[18a]</sup>

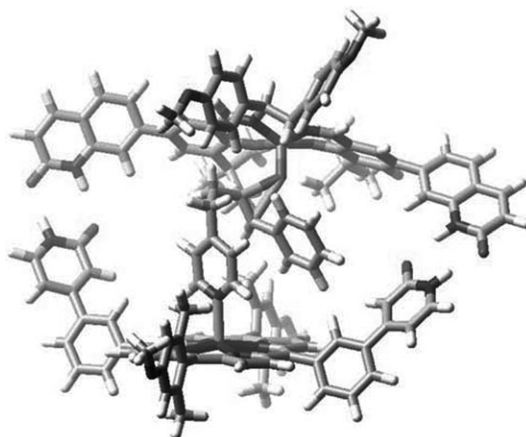


Figure 2. Molecular mechanics<sup>[21]</sup> 3D representation of the transition state of the epoxidation of a pyridine-appended styrene by **1**. Long alkyl chain substituents are removed for clarity and ease of modeling.

A model of the catalytic system **2**+**3**, the metal-free catalyst **4** and receptor **5**, was investigated by NMR dilution titrations in  $\text{CDCl}_3$  to estimate the equilibrium constants, since **2** is paramagnetic, and **2** and **3** are not soluble enough. It was clear that homopolymers of the type **4**<sub>n</sub>, **5**<sub>n</sub>, or copolymers of type **4**<sub>n</sub>**5**<sub>m</sub>, could not be neglected, since a mathematical model involving only the formation of the metal-free congener of the catalytic cyclic heterodimer **1**, the cyclic heterodimer **6** from **4**+**5** (Figures 1 and 3), could not ac-

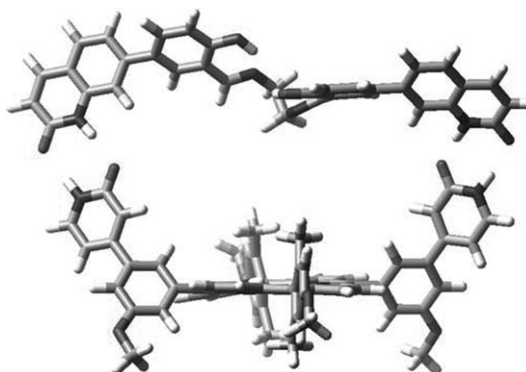


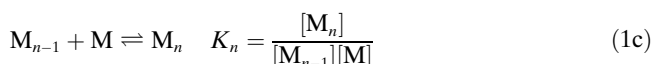
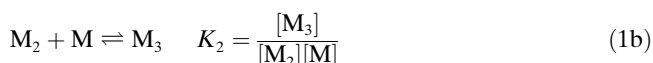
Figure 3. Molecular mechanics<sup>[21]</sup> 3D representation of the model macrocycle **6**. Long alkyl chain substituents are removed for clarity and ease of modeling.

count for the observed NMR dilution titration data (vide infra).

Thus a mathematical model was needed to account for all supramolecular polymeric species,  $4_n$ ,  $5_n$ , and  $4_n5_m$ , present in the solution of monomers **4** and **5** in addition to the discrete macrocycle **6** and the monomers themselves. We now report on the derivation of a complete association model for the formation and characterization of dynamic linear supramolecular copolymers of unlimited numbers of different monomers. This model is an extension of the isodesmic model for self-aggregation, the equal  $K$  model (EK)<sup>[15]</sup> and the covalent copolymerization model.<sup>[22]</sup> It accounts for the statistical distribution of more than one type of monomer in linear supramolecular copolymers. It is applied to the characterization of our supramolecular system described above involving formally two different monomers, **4** and **5**, but in reality three (vide infra). The model can be easily extended to also account for the simultaneous formation of cyclic species in addition to the linear copolymers, a situation commonly encountered in the field of supramolecular polymers. The technique used is (curve) fitting of an extended EK model, involving also the presence of nonlinear chemical species in the equilibrium system, to observed NMR dilution titration data at several temperatures to obtain the thermodynamic parameters,  $\Delta H^\circ$  and  $\Delta S^\circ$ , for the involved equilibria. The so-obtained thermodynamic parameters are then transformed to equilibrium constants ( $K$ ) for each measured temperature. It should be noted that (curve) fitting methods require no approximations and allow for an almost unrestricted number of experimental data points (concentrations).<sup>[12]</sup> They are correct data treatments and should produce the most reliable and accurate measurements.<sup>[12]</sup> The model is not exclusive for the area of supramolecular copolymers, but can be applied to any kinetically labile system consisting of components containing two binding sites. It should be noted that the method can be applicable to any experimental method for which the observed properties of a system consist of an average of the individual components (weighted by the mole fraction of each component).

## Results and Discussion

**Defining the association model:** Equation (1a–c) describes the equilibrium (mechanistic) model for the linear elongation of supramolecular polymers by successive addition of monomers (M) to an  $n$ -mer.



In the general case the formation of an  $n$ -mer would thus be described by  $n-1$  association constants, making the system very difficult to characterize due to the fact that to fit such a complicated model, an enormous amount of data would be required. To reduce the number of association constants, some simplified models have been developed and used with success: The EK model<sup>[15]</sup> is based on the assumption that addition of any monomer to any chain of length greater than or equal to one, takes place with the same standard free energy and therefore with the same association constant ( $K_1 = K_2 = K_3 = \dots = K_n = K_E$ ) meaning that the polymerization is non-cooperative. Another model used is the attenuated  $K$  model (AK).<sup>[15,23]</sup> In this case it is assumed that the enthalpy of addition to a growing chain is constant, while the successive addition of monomers is increasingly less probable and hence less favored entropically. As a result, the value of the association constant is tapered off ( $K_1 = K_E/2$ ;  $K_2 = K_E/3$ ;  $\dots K_n = K_E/n + 1$ ). Additional modifications of the EK model have been developed, such as assuming the first association constant to be different and all remaining association constants to be equal ( $K_1 = K_2 = K_3 = \dots = K_n = K_E$ ).<sup>[23]</sup> Another modification is to assume that the polymerization takes place up to an  $n$ -mer with the same association constant and from  $n$ -mer to higher degree of polymerization with a different association constant ( $K_{E1} = K_1 = K_2 = K_3 = \dots = K_n$ ;  $K_{E2} = K_{n+1} = K_{n+2} = K_{n+3} = \dots = K_{n+m}$ ).<sup>[24]</sup> The model that there is no energy difference between adding a monomer to another monomer or polymer is adequate for simulating most covalent polymerizations, because synthetic polymers are generally linear and incapable of nonadjacent interactions or the formation of higher order structures. Moreover, the reactivity of functional groups has long been proven to remain constant, irrelevant of the length of the chains to which they are attached.<sup>[25]</sup> This view on covalent polymerization has been the basis for the EK model of indefinite aggregation. It has been demonstrated to fit most supramolecular polymerizations.<sup>[25]</sup> Thus the simple EK model is by far the most used for supramolecular polymers.<sup>[25]</sup> This non-cooperative model should be even more applicable to systems in which there is a large spatial distance between the reacting groups in the monomers, such as in **4** and **5**, making cooperative binding by formation of tight helices less likely.

The models described above in this section are to date only developed for supramolecular polymers that have only one type of monomer, or for copolymers for which the association constants between the different monomers are equal. However, in the case in which there is more than one type of monomer, an extension of the EK model is needed. Consider for example a system consisting of three different types of monomers **a**, **b**, and **c**, each with a different, but within the same monomer, the same association element in each end. The association constants between two monomers will be all different ( $K_{aa}$ ,  $K_{bb}$ ,  $K_{cc}$ ,  $K_{ab}$ ,  $K_{ac}$ , and  $K_{bc}$ , Figure 4), but in this extended EK model, a specific association constant between two given monomers will not change if the location of these two monomers changes within a

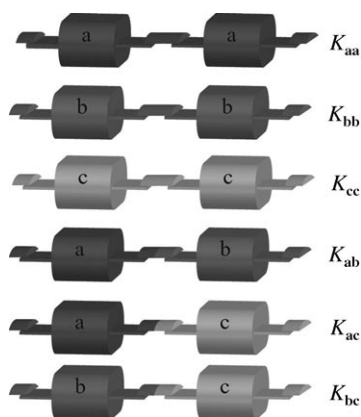


Figure 4. Representation of the different associations between different monomers **a**, **b** and **c**.

supramolecular copolymer. Still, the derivation of the EK model becomes complicated. In fact, the general extensions that exist consider systems of two monomers only and in addition, the derivations are made in ways that do not generalize to higher dimensional systems as stated above.<sup>[13]</sup> However, as will be demonstrate here, the EK model can be extended to any situation by the stringent use of linear algebra. Our approach is related to a framework found in Chapter III of Flory's book "Statistical Mechanism for Chain Molecules",<sup>[22]</sup> and it is also similar to computations done for so-called hidden Markov models in statistics.<sup>[26]</sup> The only limitation in the application of the model is caused by the restricted number of experimental data.

### Derivation of the mathematical model

**General notations:** Consider a system comprising  $r$  different types of monomers, and let  $\mathcal{M}$  be the set of all monomers. Let  $\mathbf{M}$  be an  $r \times r$  matrix, the  $(x, y)$  element (row  $x$ , column  $y$ ) of which is  $K_{xy}c_x$ , in which  $x$  and  $y$  are two types of monomers (possibly  $x = y$ ),  $c_x$  is the concentration of unbound monomer  $x$  and  $K_{xy}$  is the association constant for the interaction between monomers  $x$  and  $y$  [Eq. (2)]. Further, if we define  $\mathbf{K}$  as the matrix with the association constants  $K_{xy}$  as elements and  $\Delta_c$  as the diagonal matrix with the concentrations  $c_x$  of unbound monomers as elements, then  $\mathbf{M} = \mathbf{K}\Delta_c$ . Finally let  $\mathbf{c}$  denote the column vector of all elements  $c_x$ , let  $\mathbf{1}$  denote the  $r \times 1$  vector of all ones and let  $\mathbf{1}_x$  denote the  $r \times 1$  vector the  $x$ -th element of which is one, while its remaining elements are zero. The different matrices will be exemplified in the case study: the supramolecular system **4+5** and its components (vide infra).



**Derivation of the mass-balance equations:** The total concentration of any species, monomers or polymers, is denoted by  $T$ , and the concentration of specific species, like unbounded monomers or a specific polymer of length  $n$ , is denoted by  $c$ .

To estimate the different parameters that characterize a supramolecular polymer, we need to estimate the association constants. The first step will be to solve the mass-balance equation for the concentrations ( $c_x$ ) of unbound monomers. These values can then be used to fit the model to the experimental data, giving the estimated association constants. The association constants can, in turn, be used to compute for example the average degree of polymerization (DP) or the mole fractions for a specific monomer in different environments, for instance adjacent to the same type of monomer, to exactly one monomer of the same type or to two monomers of different type. However, for clarity, the total concentration of polymers,  $T_{\text{polymer}}$ , is first computed and then different constraints will be added to obtain the total concentration,  $T_x$ , of specific monomers.

For a copolymer consisting of three monomers **a**, **b**, and **c**, the mass balance  $T_a$  of monomer **a** can be expressed as Equation (3).

$$T_a = \sum_{n=1}^{\infty} \sum_{m=0}^{\infty} \sum_{k=0}^{\infty} n c_{a_n b_m c_k} \quad (3)$$

Equation (3) can be difficult to express when the association constants  $K_{aa}$ ,  $K_{bb}$ ,  $K_{cc}$ ,  $K_{ab}$ ,  $K_{ac}$ , and  $K_{bc}$  are different, since all possible successions of association constants between monomers in the chain. However, consider a polymer named **p** of length  $n$  and define  $p_k$  as the monomer at position  $k$  in **p**, and  $K_{p_{k-1}p_k}$  as the association constant between the monomers at positions  $k-1$  and  $k$ . The concentration of **p**,  $c_p$ , can then be expressed as Equation (4) in which  $c_{p_k}$  is the corresponding unbound concentration of the specific monomer at position  $k$  in **p**.

$$\begin{aligned} c_p &= c_{p_1} K_{p_1 p_2} c_{p_2} \dots K_{p_{n-1} p_n} c_{p_n} = c_{p_1} \prod_{k=2}^n K_{p_{k-1} p_k} c_{p_k} \\ &= c_{p_1} \prod_{k=2}^n M_{p_{k-1} p_k} \end{aligned} \quad (4)$$

The total concentration of all polymers of length  $n$ , denoted by  $c_n$ , is obtained by summing Equation (4) over all polymers of length  $n$ , that is, over all sequences **p** in the product set  $\mathcal{M}^n = \mathcal{M} \times \mathcal{M} \times \dots \times \mathcal{M}$ . We can write this sum as Equation (5) in which the superindex T denotes matrix transposition and the second equality is a result of the very definition of a matrix product.

$$c_n = \sum_{\mathbf{p} \in \mathcal{M}^n} c_{p_1} \prod_{k=2}^n M_{p_{k-1} p_k} = \mathbf{c}^T \mathbf{M}^{n-1} \mathbf{1} \quad (5)$$

The total concentration of *all* polymers is given by Equation (6) in which  $\mathbf{I}$  is the identity matrix.

$$\begin{aligned} T_{\text{polymers}} &= \sum_{n=1}^{\infty} c_n = \sum_{n=1}^{\infty} \mathbf{c}^T \mathbf{M}^{n-1} \mathbf{1} = \mathbf{c}^T (\mathbf{I} - \mathbf{M})^{-1} \mathbf{1} \\ &= \mathbf{1}^T (\Delta_c^{-1} - \mathbf{K})^{-1} \mathbf{1} \end{aligned} \quad (6)$$

For the sum to converge, it is sufficient that the spectral radius of  $\mathbf{M}$ , that is, the largest moduli of its eigenvalues is less than one. This criterion thus guarantees that the system will be stable. The right-hand side of the above equation highlights the symmetry of the expression (both  $\Delta_c$  and  $\mathbf{K}$  are symmetric matrices); this final equality follows by writing  $\mathbf{I} = \Delta_c^{-1} \Delta_c$  to see that  $(\mathbf{I} - \mathbf{M})^{-1} = \Delta_c^{-1} (\Delta_c^{-1} - \mathbf{K})^{-1}$  and then noting that  $\Delta_c^{-1}$  is simply the diagonal matrix of reciprocals  $c_x^{-1}$ .

The total concentration of all monomers in solution and associated in polymers can be obtained similarly, by multiplying (weighting) the concentration of polymers of length  $n$  by the number  $n$  of monomers in such polymers. Thus we arrive at Equation (7).

$$\begin{aligned} T_{\text{monomers}} &= \sum_{n=1}^{\infty} n \mathbf{c}^T \mathbf{M}^{n-1} \mathbf{1} \\ &= \mathbf{c}^T (\mathbf{I} - \mathbf{M})^{-2} \mathbf{1} \\ &= \mathbf{1}^T (\Delta_c^{-1} - \mathbf{K})^{-1} \Delta_c^{-1} (\Delta_c^{-1} - \mathbf{K})^{-1} \mathbf{1} \end{aligned} \quad (7)$$

If we now look for a specific monomer ( $x$ ) at a specific position ( $s$ ) in any polymer of length  $n$ , we can express the total concentration  $c_n^{x,s}$  of polymers of length  $n$ , having monomer  $x$  at position  $s$  as Equation (8).

$$c_n^{x,s} = \sum_{\mathbf{p} \in \mathcal{H}^n; p_s = x} c_{p_1} \prod_{k=2}^n M_{p_{k-1} p_k} = \mathbf{c}^T \mathbf{M}^{s-1} \mathbf{1}_x \mathbf{1}_x^T \mathbf{M}^{n-1} \mathbf{1} \quad (8)$$

Here the sum is taken over all length  $n$  polymers that have monomer  $x$  position  $s$ ; indeed, the matrix  $\mathbf{1}_x \mathbf{1}_x^T$ , which has a single non-zero entry equal to one at position  $(s, s)$ , picks out those polymers for which  $p_s = x$  from the set of all length- $n$  polymers. Summing Equation (8) over all  $n \geq s$  gives the total concentration of polymers with monomer  $x$  at position  $s$  as Equation (9).<sup>[27]</sup>

$$\begin{aligned} c_x^{s,s} &= \sum_{n=s}^{\infty} \mathbf{c}^T \mathbf{M}^{s-1} \mathbf{1}_x \mathbf{1}_x^T \mathbf{M}^{n-s} \mathbf{1} \\ &= \mathbf{c}^T \mathbf{M}^{s-1} \mathbf{1}_x \mathbf{1}_x^T (\mathbf{I} - \mathbf{M})^{-1} \mathbf{1} \\ &= \mathbf{c}^T \mathbf{M}^{s-1} \mathbf{1}_x c_x^{-1} \mathbf{1}_x^T (\Delta_c^{-1} - \mathbf{K})^{-1} \mathbf{1} \end{aligned} \quad (9)$$

Summing over all  $s \geq 1$ , we obtain the total concentration of monomer  $x$  in the system (unbound or bound anywhere in any polymer of any length) as Equation (10).<sup>[28]</sup>

$$\begin{aligned} T_x &= \sum_{n=1}^{\infty} \mathbf{c}^T \mathbf{M}^{s-1} \mathbf{1}_x c_x^{-1} \mathbf{1}_x^T (\Delta_c^{-1} - \mathbf{K})^{-1} \mathbf{1} \\ &= \mathbf{c}^T (\mathbf{I} - \mathbf{M})^{-1} \mathbf{1}_x c_x^{-1} \mathbf{1}_x^T (\Delta_c^{-1} - \mathbf{K})^{-1} \mathbf{1} \\ &= \mathbf{1}^T (\Delta_c^{-1} - \mathbf{K})^{-1} \mathbf{1}_x c_x^{-1} \mathbf{1}_x^T (\Delta_c^{-1} - \mathbf{K})^{-1} \mathbf{1} \\ &= c_x^{-1} (\mathbf{1}^T (\Delta_c^{-1} - \mathbf{K})^{-1} \mathbf{1}_x)^2 \end{aligned} \quad (10)$$

For a single type monomer system ( $r=1$ ), containing monomer  $M$ , Equation (10) reduces to the standard EK model relation<sup>[15]</sup> with the matrices  $\mathbf{K} = (K_E)$  and  $\Delta_c = (c_M)$

given in Equation (11).

$$T_M = c_M^{-1} (c_M^{-1} - K_E)^{-2} = \frac{c_M}{(1 - K_E c_M)^2} \quad (11)$$

*Derivation of parameters related to the composition of all supramolecular copolymers in solution:* The degree of polymerization is defined as the number of monomeric units in a chain. The average degree of polymerization (DP), is defined as the average number of monomeric units in polymer assemblies. It is given by

$$\overline{\text{DP}} = \frac{\text{number of monomers}}{\text{number of assemblies}}$$

Recalling that Equation (6) gives the total concentration of all supramolecular polymers in solution and that Equation (7) gives the total concentration of all monomers, we can compute the degree of polymerization as Equation (12).

$$\overline{\text{DP}} = \frac{T_{\text{monomers}}}{T_{\text{polymers}}} = \frac{\mathbf{1}^T (\Delta_c^{-1} - \mathbf{K})^{-1} \Delta_c^{-1} (\Delta_c^{-1} - \mathbf{K})^{-1} \mathbf{1}}{\mathbf{1}^T (\Delta_c^{-1} - \mathbf{K})^{-1} \mathbf{1}} \quad (12)$$

For a single type monomer system ( $r=1$ ), containing monomer  $M$ , Equation (12) reduces to the standard EK model relation [Eq. (13)],<sup>[24]</sup> with the matrices  $\mathbf{K} = (K_E)$  and  $\Delta_c = (c_M)$ .

$$\overline{\text{DP}} = \frac{1}{1 - K_E c_M} \quad (13)$$

Other parameters related to the composition of all polymers in the system can be calculated, as for example the mole fraction of specific monomer in polymers [Eq. (14)], or (case 1) the mole fraction of monomers adjacent to identical monomers [Eq. (15)], or (case 2) that of exactly one adjacent monomer of different type [Eq. (16)], or (case 3) that of two adjacent monomers of different type [Eq. (17)].

$$\chi_x^{\text{polymers}} = \frac{c_x^{\text{polymers}}}{T_x} \quad (14)$$

$$\chi_x^{(1)} = \frac{c_x^{(1)}}{T_x} \quad (15)$$

$$\chi_x^{(2)} = \frac{c_x^{(2)}}{T_x} \quad (16)$$

$$\chi_x^{(3)} = \frac{c_x^{(3)}}{T_x} \quad (17)$$

The concentration of a specific monomer in all polymers of length  $n > 1$  can be calculated by subtracting the free concentration of this monomer from its total concentration. By using Equation (10), this can be expressed as Equation (18).

$$c_x^{\text{polymers}} = T_x - c_x = c_x^{-1} (\mathbf{1}^T (\Delta_c^{-1} - \mathbf{K})^{-1} \mathbf{1}_x)^2 - c_x \quad (18)$$

On the other hand to obtain the other mole fractions, as defined in Equations (15)–(17), it will be necessary to find expressions for the concentration of monomers  $x$  in the system having  $y$  next to itself (pair  $xy$ ), and even triplets ( $yxz$ ). If we choose two monomers denoted  $x$  and  $y$  ( $x$  and  $y$  can be identical), we have a pair of monomers  $xy$  in a chain in this order, whenever the monomer at a position  $s$  is  $y$  and that at position  $s-1$  is  $x$  (hence  $2 \leq s \leq n$ ). The concentration of polymers  $\mathbf{p}$  of length  $n$  having such a pair at position  $s$  can be written as Equation (19).

$$c_n^{x,y;s} = \sum_{\mathbf{p} \in \mathcal{M}^n; p_{s-1}=x, p_s=y} c_{p_1} \prod_{k=2}^n M_{p_{k-1}p_k} = \mathbf{c}^T \mathbf{M}^{s-2} \mathbf{1}_x M_{xy} \mathbf{1}_y^T \mathbf{M}^{n-s} \mathbf{1} \quad (19)$$

This computation is similar to Equation (8) in that the summation is taken over a specific subset of the set of polymers of length  $n$ ; here the subset is those polymers that have monomers  $x$  and  $y$  at positions  $s-1$  and  $s$  respectively. Summing Equation (19) over all  $n \geq s$  and then over all  $s \geq 2$ , we obtain the total concentration of pairs of monomers  $xy$  in the system as Equation (20).

$$\begin{aligned} c^{x,y} &= \sum_{s=2}^{\infty} \sum_{n=s}^{\infty} \mathbf{c}^T \mathbf{M}^{s-2} \mathbf{1}_x M_{xy} \mathbf{1}_y^T \mathbf{M}^{n-s} \mathbf{1} \\ &= \mathbf{c}^T (\mathbf{I} - \mathbf{M})^{-1} \mathbf{1}_x M_{xy} \mathbf{1}_y^T (\mathbf{I} - \mathbf{M})^{-1} \mathbf{1} \\ &= \mathbf{1}^T (\Delta_c^{-1} - \mathbf{K})^{-1} \mathbf{1}_x K_{xy} \mathbf{1}_y^T (\Delta_c^{-1} - \mathbf{K})^{-1} \mathbf{1} \end{aligned} \quad (20)$$

We now want to calculate the concentration of monomers  $x$  in a polymer  $\mathbf{p}$  that are adjacent to monomers of type  $y$  and  $z$  ( $y$  and  $z$  can be of different type from  $x$ ) in the order of  $yxz$ . Consider a polymer  $\mathbf{p}$  of length  $n \geq 3$  and a position  $1 < s < n-1$ . The concentration of such polymers with  $p_{s-1} = y$ ,  $p_s = x$ , and  $p_{s+1} = z$  is given by Equation (21).

$$\begin{aligned} c_n^{y,x,z;s} &= \sum_{\mathbf{p} \in \mathcal{M}^n; p_{s-1}=y, p_s=x, p_{s+1}=z} c_{p_1} \prod_{k=2}^n M_{p_{k-1}p_k} \\ &= \mathbf{c}^T \mathbf{M}^{s-2} \mathbf{1}_y M_{yx} M_{xz} \mathbf{1}_z^T \mathbf{M}^{n-s-1} \mathbf{1} \end{aligned} \quad (21)$$

Summing Equation (21) first over  $n \geq s+1$  and then over  $s \geq 2$  gives the concentration of triplets  $xyz$  in all polymers as Equation (22).

$$\begin{aligned} c^{y,x,z} &= \sum_{s=2}^{\infty} \sum_{n=s+1}^{\infty} c_n^{y,x,z;s} \\ &= \mathbf{c}^T (\mathbf{I} - \mathbf{M})^{-1} \mathbf{1}_y M_{yx} M_{xz} \mathbf{1}_z^T (\mathbf{I} - \mathbf{M})^{-1} \mathbf{1} \\ &= \mathbf{1}^T (\Delta_c^{-1} - \mathbf{K})^{-1} \mathbf{1}_y K_{yx} c_x K_{xz} \mathbf{1}_z^T (\Delta_c^{-1} - \mathbf{K})^{-1} \mathbf{1} \end{aligned} \quad (22)$$

**Case 1:** There are two contributions to account for having a monomer adjacent to the same type of monomer: one contribution when the monomer is at the end of a chain and one when it is in the interior of a chain.

For the first contribution, we look at the monomer at the end of a chain of length equal to or greater than 2 ( $n \geq 2$ ).

Using Equation (19) with  $s=2$ , we obtain the concentration of polymers of length  $n$  for which the monomers at positions one and two are identical and equal to  $x$  [Eq. (23)].

$$c_n^{x,x;2} = \mathbf{c}^T \mathbf{1}_x M_{xx} \mathbf{1}_x^T \mathbf{M}^{n-2} \mathbf{1} = c_x M_{xx} \mathbf{1}_x^T \mathbf{M}^{n-2} \mathbf{1} \quad (23)$$

By symmetry, the concentration of polymers in which the two last monomers are identical and equal to  $x$  is the same. By summing Equation (23) over all  $n \geq 2$  we obtain the total concentration of polymers in which the two first monomers are  $x$ , as Equation (24).

$$c^{x,x;2} = \sum_{n=2}^{\infty} c_n^{x,x;2} = c_x M_{xx} \mathbf{1}_x^T (\mathbf{I} - \mathbf{M})^{-1} \mathbf{1} = c_x K_{xx} \mathbf{1}_x^T (\Delta_c^{-1} - \mathbf{K})^{-1} \mathbf{1} \quad (24)$$

For the second contribution, we look at triplet  $xyz$  when  $y=x$  and  $z=x$ . This can be computed from Equation (25), based on Equation (22).

$$c^{x,x,x} = \mathbf{1}^T (\Delta_c^{-1} - \mathbf{K})^{-1} \mathbf{1}_x K_{xx} c_x K_{xx} \mathbf{1}_x^T (\Delta_c^{-1} - \mathbf{K})^{-1} \mathbf{1} \quad (25)$$

Summing up the two kinds of contributions, we find that the total concentration of monomer  $x$  adjacent to the same type of monomer in all polymers is given by Equation (26).

$$c_x^{(1)} = 2c_x K_{xx} \mathbf{1}_x^T (\Delta_c^{-1} - \mathbf{K})^{-1} \mathbf{1} + c_x K_{xx}^2 (\mathbf{1}_x^T (\Delta_c^{-1} - \mathbf{K})^{-1} \mathbf{1})^2 \quad (26)$$

**Case 2:** Again there are two different contributions to account for having a monomer adjacent to exactly one monomer of different type: when it is at the first or last position of a chain and when it is in the interior.

The first contribution can be computed by considering a polymer of length  $n \geq 2$ . The concentration of such polymers for which the first monomer is  $x$  and the second is different (denoted  $y$ ) is computed from Equation (19) with  $s=2$  as Equation (27).

$$c_n^{x \neq x;2} = \sum_{y \neq x} \mathbf{c}^T \mathbf{1}_x M_{xy} \mathbf{1}_y^T \mathbf{M}^{n-2} \mathbf{1} = \sum_{y \neq x} c_x M_{xy} \mathbf{1}_y^T \mathbf{M}^{n-2} \mathbf{1} \quad (27)$$

Summing this up over  $n \geq 2$  gives the total concentration of polymers for which the first monomer is  $x$  and the second is different as Equation (28), in which  $\mathbf{K}_{\neq x,x}$  is column  $x$  of  $\mathbf{K}$ , with its  $x$ -th element replaced by 0. By symmetry, the concentration of polymers for which the two last monomers are not identical and the last monomer is  $x$ , is the same.

$$\begin{aligned} c^{x \neq x} &= \sum_{n=2}^{\infty} \sum_{y \neq x} c_n^{x \neq x;2} \\ &= \sum_{y \neq x} c_x M_{xy} \mathbf{1}_y^T (\mathbf{I} - \mathbf{M})^{-1} \mathbf{1} \\ &= \sum_{y \neq x} c_x K_{xy} \mathbf{1}_y^T (\Delta_c^{-1} - \mathbf{K})^{-1} \mathbf{1} \\ &= c_x \mathbf{K}_{\neq x,x}^T (\Delta_c^{-1} - \mathbf{K})^{-1} \mathbf{1} \end{aligned} \quad (28)$$

The other contribution can be computed from Equation (22) with  $y=x$  and  $z \neq x$ , or  $y \neq x$  and  $z=x$  [Eq. (29)].

$$c^{x,x,y,y,x,x} = \sum_{y \neq x} \mathbf{1}^T (\Delta_c^{-1} - \mathbf{K})^{-1} \mathbf{1}_x K_{xx} c_x K_{xy} \mathbf{1}_y^T (\Delta_c^{-1} - \mathbf{K})^{-1} \mathbf{1} + \sum_{y \neq x} \mathbf{1}^T (\Delta_c^{-1} - \mathbf{K})^{-1} \mathbf{1}_y K_{yx} c_x K_{xx} \mathbf{1}_x^T (\Delta_c^{-1} - \mathbf{K})^{-1} \mathbf{1} \quad (29) \\ = 2c_x K_{xx} \mathbf{1}^T (\Delta_c^{-1} - \mathbf{K})^{-1} \mathbf{1}_x K_{x,\neq x}^T (\Delta_c^{-1} - \mathbf{K})^{-1} \mathbf{1}$$

Summing the two kinds of contributions, we find that the total concentration of monomer  $x$  adjacent to exactly one monomer of different type in all polymers is given by Equation (30).

$$c_x^{(2)} = 2c_x K_{\neq x,x}^T (\Delta_c^{-1} - \mathbf{K})^{-1} \mathbf{1} + 2c_x K_{xx} \mathbf{1}^T (\Delta_c^{-1} - \mathbf{K})^{-1} \mathbf{1}_x K_{x,\neq x}^T (\Delta_c^{-1} - \mathbf{K})^{-1} \mathbf{1} \quad (30)$$

*Case 3:* In this case there is only one contribution to account for having a monomer adjacent to two monomers of different type. From Equation (22), we compute the concentration of monomers  $x$  that have two adjacent monomers of type different from  $x$  with  $y \neq x$  and  $z \neq x$  as Equation (31).

$$c_x^{(3)} = \sum_{y \neq x} \sum_{z \neq x} \mathbf{1}^T (\Delta_c^{-1} - \mathbf{K})^{-1} \mathbf{1}_y K_{yx} c_x K_{xz} \mathbf{1}_z^T (\Delta_c^{-1} - \mathbf{K})^{-1} \mathbf{1} \\ = \mathbf{1}^T (\Delta_c^{-1} - \mathbf{K})^{-1} \mathbf{K}_{\neq x,x} c_x \mathbf{K}_{\neq x,x}^T (\Delta_c^{-1} - \mathbf{K})^{-1} \mathbf{1} \quad (31) \\ = c_x (\mathbf{K}_{\neq x,x}^T (\Delta_c^{-1} - \mathbf{K})^{-1} \mathbf{1})^2$$

*Derivation of a general expression for the determination of association constants by NMR titrations for supramolecular copolymers containing monomers with two binding sites:* One way to estimate equilibrium constants is to use NMR titrations.<sup>[12]</sup> Indeed, when the kinetics of the equilibrium is faster than the NMR timescale, the observed chemical shift of a specific proton resonance is an average of the resonances of this proton in unbound and bound species, weighted by the mole fractions of the different states present in solution. For a process such as dimerization or polymerization of a molecule, the chemical shifts become concentration-dependent because the mole fractions of the different states are directly related to the total concentration of each monomer.

Since for any monomer  $x$  in a linear supramolecular polymer there are two binding sites, the chemical shift of a particular resonance of a particular monomer will be the sum of the chemical shifts for the various states of its binding sites weighted by the concentration of sites in the respective states relative to the total concentration of sites. A binding site can be either free (free sites), bound to the same type of monomer ( $x$  to  $x$ ) or to a different type of monomer ( $x$  to  $y$ ) in a copolymer. Thus, if we consider a supramolecular polymer composed of more than one type of monomers, the chemical shift of the proton resonances for any monomer  $x$ ,  $\delta_{H_x}$ , can be taken from the expressions given in Equations (32)–(35).

$$\delta_{H_x} = \chi_x^{\text{free sites}} \delta_{H_x}^{\text{free}} + \chi_x^{x \text{ to } x} \delta_{H_x}^{xx} + \sum_{y \neq x} \chi_x^{x \text{ to } y} \delta_{H_x}^{xy} \quad (32)$$

$$\chi_x^{\text{free sites}} = \frac{c^{\text{free sites}}}{T_{\text{sites } x}} \quad (33)$$

$$\chi_x^{x \text{ to } x} = \frac{c^{x \text{ to } x}}{T_{\text{sites } x}} \quad (34)$$

$$\chi_x^{x \text{ to } y} = \frac{c^{x \text{ to } y}}{T_{\text{sites } x}} \quad (35)$$

Since each monomer  $x$  is defined to contain two identical binding sites (see Figure 4), the total concentration ( $T_{\text{sites } x}$ ) of binding sites is equal to twice the total concentration ( $T_x$ ) of the monomer  $x$  added to the solution.

First we compute the concentration of unbound binding sites ( $c^{\text{free sites}}$ ) for a specific monomer  $x$ . A monomer has a free binding site if it is situated at the first or last position of any polymer of length  $n \geq 1$ . Using Equation (8) with  $s=1$  and  $s=n$ , we can compute the concentration of polymers of length  $n$  for which the first or last monomer is  $x$ . Then summing up over all  $n \geq 1$  we obtain the total concentration of polymers for which the first or last monomer is  $x$ , which represents the concentration of free binding sites [Eq. (36)].

$$c_x^{\text{free sites}} = \sum_{n=1}^{\infty} c_n^{x:1} + \sum_{n=1}^{\infty} c_n^{x:n} \\ = \sum_{n=1}^{\infty} \mathbf{c}^T \mathbf{1}_x \mathbf{1}_x^T \mathbf{M}^{n-1} \mathbf{1} + \sum_{n=1}^{\infty} \mathbf{c}^T \mathbf{M}^{n-1} \mathbf{1}_x \mathbf{1}_x^T \mathbf{1} \quad (36) \\ = 2\mathbf{c}^T \mathbf{1}_x \mathbf{1}_x^T (\mathbf{I} - \mathbf{M})^{-1} \mathbf{1} \\ = 2 \times \mathbf{1}_x^T (\Delta_c^{-1} - \mathbf{K})^{-1} \mathbf{1}$$

To compute the concentration  $c^{x \text{ to } y}$  of binding sites of monomers  $x$  bound to a binding site of monomer  $y$ , we have to consider two different contributions; either we have the pair  $xy$  ( $y$  at position  $s$  and  $x$  at position  $s-1$ ,  $c^{x,y}$ ) or the other way around,  $yx$  ( $c^{y,x}$ ). Using Equation (20) for the two cases we obtain the concentration of binding sites  $x$  to  $y$  in all polymers as Equation (37).

$$c^{x \text{ to } y} = c^{x,y} + c^{y,x} \\ = \mathbf{1}^T (\Delta_c^{-1} - \mathbf{K})^{-1} \mathbf{1}_x K_{xy} \mathbf{1}_y^T (\Delta_c^{-1} - \mathbf{K})^{-1} \mathbf{1} \\ + \mathbf{1}^T (\Delta_c^{-1} - \mathbf{K})^{-1} \mathbf{1}_y K_{yx} \mathbf{1}_x^T (\Delta_c^{-1} - \mathbf{K})^{-1} \mathbf{1} \quad (37) \\ = 2 \times \mathbf{1}^T (\Delta_c^{-1} - \mathbf{K})^{-1} \mathbf{1}_x K_{xy} \mathbf{1}_y^T (\Delta_c^{-1} - \mathbf{K})^{-1} \mathbf{1}$$

Equation (37) can be used to compute the concentration of binding sites bound to the same type in all polymers ( $c^{x \text{ to } x}$ ) with  $x=y$  [Eq. (38)].

$$c^{x \text{ to } x} = 2 \times \mathbf{1}^T (\Delta_c^{-1} - \mathbf{K})^{-1} \mathbf{1}_x K_{xx} \mathbf{1}_x^T (\Delta_c^{-1} - \mathbf{K})^{-1} \mathbf{1} \quad (38)$$

Inserting Equations (36)–(38) into Equations (32)–(35) gives the expression [Eq. (39)] that relates the observed ex-



perimental data  $\delta_{H_x}$  to the unknown association constants and the concentrations of unbound monomers as expressed by the matrices  $\mathbf{K}$  and  $\Delta_c$ , respectively.

$$\delta_{H_x} = \frac{2 \times \mathbf{1}_x^T (\Delta_c^{-1} - \mathbf{K})^{-1} \mathbf{1}}{T_{\text{sites } x}} \delta^{\text{free}} + \frac{2 \times \mathbf{1}_x^T (\Delta_c^{-1} - \mathbf{K})^{-1} \mathbf{1}_x K_{xx} \mathbf{1}_x^T (\Delta_c^{-1} - \mathbf{K})^{-1}}{T_{\text{sites } x}} \delta_{H_x}^{xx} + \sum_{y \neq x} \frac{2 \times \mathbf{1}_x^T (\Delta_c^{-1} - \mathbf{K})^{-1} \mathbf{1}_x K_{xy} \mathbf{1}_y^T (\Delta_c^{-1} - \mathbf{K})^{-1}}{T_{\text{sites } x}} \delta_{H_x}^{xy} \quad (39)$$

### Application of the mathematical model on the supramolecular system 4+5

*Definition of the system used in the case study:* Including linear polymers of salen **4** and porphyrin **5** (structures in Figure 1) to the preliminary association model  $4+5=6$ <sup>[18a]</sup> did not provide a good fit to experimental NMR data obtained in CDCl<sub>3</sub>. A breakthrough was made when a sample of **5** was recorded on a <sup>1</sup>H NMR spectrometer at a frequency of 500 MHz instead of at lower frequencies. The <sup>1</sup>H NMR spectra of **5** at 500 MHz show the presence of two different species. They have the same structure since all resonances are duplicated, except for the resonances of the two methyl groups on each benzene ring at positions 10 and 20 of **5**, which appear as three singlets. This behavior can only be explained by the presence of two different atropisomers of **5**, one having a *cisoid* conformation, **5c**, and the other a *transoid*, **5t**. For **5c**, the two sides of the porphyrin plane are not identical (Figure 5a), which gives rise to two magnetically

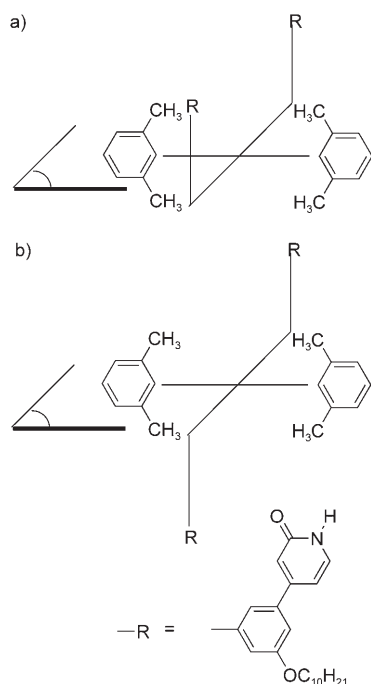


Figure 5. Schematic representation of the different atropisomers, a) **5c** and b) **5t** of porphyrin **5**.

different environments for the two methyl groups, one above the plane and one below. In contrast, for **5t**, the two sides of the porphyrin plane are identical (Figure 5b). The protons of the two methyl groups are thus magnetically identical, giving rise to only one resonance in the <sup>1</sup>H NMR spectrum.

Also intriguing is that the chemical shift of the NH proton resonance of the 2-pyridone moiety is concentration-dependent for both **5c** and **5t**. However, the shift of the above-mentioned proton resonance of **5t** is more sensitive to the variation of the total concentration of **5** (Figure 6, middle), indicating that **5c** and **5t** are not exclusively involved in the same type of associations. The chemical shift of the NH proton resonance of the 2-pyridone moiety of **5c** is closer to the chemical shift at highest concentration over the concentration range, in which the chemical shift is closest to the one of full association. Therefore, it seems likely that **5c** must be involved in formation of additional more well-defined complexes compared to **5t**, in addition to the mutual complexes involving both **5c** and **5t**.

Computational modeling<sup>[21]</sup> showed that **5c** can form a cyclic trimer, **7** (Figure 7) in the equilibrium mixture. This result is not surprising due to the spatial orientation of the two 2-pyridone moieties in **5** (120°) and the ability of the latter to rotate freely around the phenylene–(2-pyridone) bond to find an angle to bind to the 2-pyridone moiety of a neighboring **5**. This mechanism is similar to the formation of cyclic dimers in addition to linear polymers for bis(2-pyridone) rods in which the two 2-pyridone moieties are at 180° spatial orientation to each other.<sup>[29]</sup> The formation of **7** implies that the chemical shift of the 2-pyridone NH proton resonance for **5c** is an average weighted by the mole fractions of **5c** present in **7**, polymers, and as a free species, while in **5t** the corresponding chemical shift is only the average of **5t** as a free species and as a component of supramolecular polymers. A direct observation of the cyclic trimer **7** in the present system is difficult due to the fact that it exists in a small amount and that it is in fast equilibrium with other similar species, precluding direct isolation or spectroscopic identification including DOSY.<sup>[11]</sup> ESIMS could indeed identify trimers, but will not be able to confirm that they are cyclic.<sup>[30,31]</sup>

For salen **4**, the <sup>1</sup>H NMR spectra are as expected; salen **4** shows only one type of conformer (Figure 6 (top) shows the part containing the 2-quinolone NH proton resonance), since the multiplicity of all the observed resonances were as predicted from one structure. The resonance of the 2-quinolone NH proton was the only one demonstrating large concentration dependence. As a result, in the <sup>1</sup>H NMR dilution titrations of **4+5** (Figure 6, bottom), the chemical shift of three NH proton resonances from the 2-pyridone motifs were followed, one for **4** and two for **5**; thus the term “formally a two-component system, in reality a three-component” is used to describe the supramolecular system **4+5**.

For system **4+5**, all involved equilibrium constants can now be defined: In addition to the association constants for the elongation of the supramolecular polymers [ $K_{44}$ ,  $K_{55}$ ,

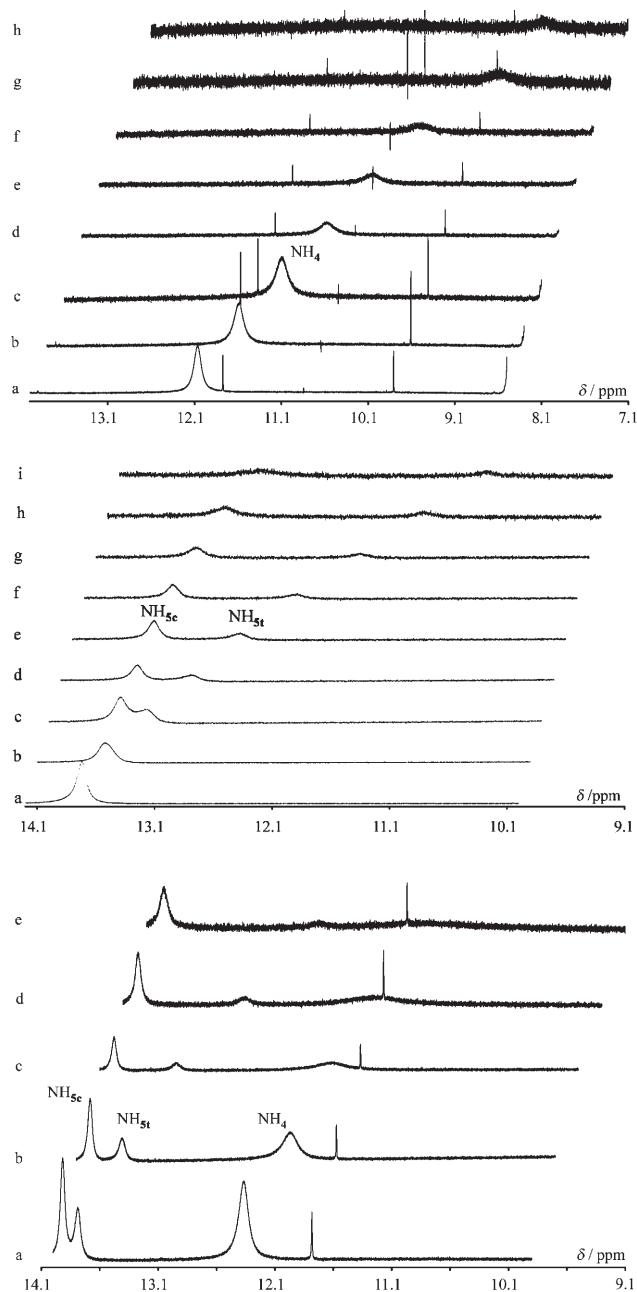


Figure 6. Top: A part of the  $^1\text{H}$  NMR spectra (500 MHz,  $\text{CDCl}_3$ , 283 K) of **4** at  $T_4 =$  a) 30, b) 18, c) 10.1, d) 6.5, e) 3.9, f) 2.3, g) 1.4, and h) 0.50 mm. Middle: A part of the  $^1\text{H}$  NMR spectra (500 MHz,  $\text{CDCl}_3$ , 283 K) of **5** at  $T_5 =$  a) 30, b) 18, c) 10.1, d) 6.5, e) 3.9, f) 2.3, g) 1.4, h) 0.80, and i) 0.50 mm. Bottom: A part of the  $^1\text{H}$  NMR spectra (500 MHz,  $\text{CDCl}_3$ , 283 K) of system **4+5** at  $T_4 = T_5 =$  a) 15.2, b) 8.1, c) 4.3, d) 2.3, and e) 1.2 mm.

$K_{45}$ , Eq. (40)], we have the equilibrium constant for the formation of the heterodimer **6** from a linear dimer composed of **4** and **5c** [ $K_6$ , Eq. (41)]. Finally we have the equilibrium constant for the formation of the cyclic trimer **7** from the linear trimer composed of three **5c** [ $K_7$ , Eq. (42)] and the equilibrium constant for the isomerization of the *transoid* atropisomer **5t** to the *cisoid* **5c** [ $K_i$ , Eq. (43)].

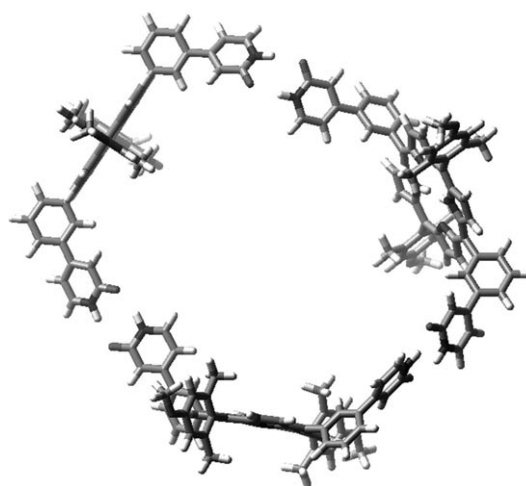
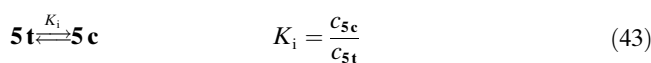
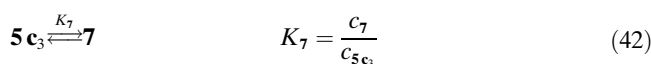
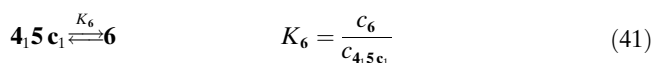
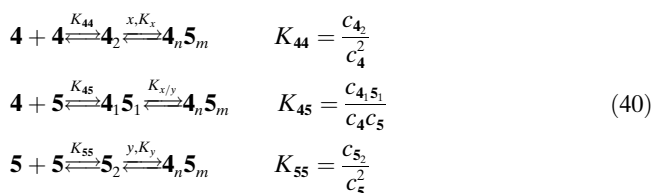


Figure 7. Molecular mechanics<sup>[21]</sup> 3D representation of cyclic trimer **7**. Long alkyl chain substituents are removed for clarity and ease of modeling.



There are nine chemical shifts defined for the system (Figure 8). For salen **4** there are four different chemical shifts for the resonance of the 2-quinolone NH: one for the 2-quinolone binding unit when it is free ( $\delta_4^{\text{free}}$ ), another when it is hydrogen bonded to the same type of monomer in a chain ( $\delta_4^{44}$ ), one when it is hydrogen bonded to a monomer of different type in a chain ( $\delta_4^{45}$ ), and finally one when it is hydrogen bonded to **5c** in heterodimer **6** ( $\delta_4^6$ ). The same applies to porphyrin **5**: one when it is free ( $\delta_5^{\text{free}}$ ), one when it is hydrogen bonded to the same type of monomer ( $\delta_5^{55}$ ), one when it is hydrogen bonded to a monomer of different type in a chain ( $\delta_5^{45}$ ) and one when **5c** is hydrogen bonded to **4** in heterodimer **6** ( $\delta_5^6$ ). However, for **5** we have one more chemical shift, since **5c** can form the cyclic trimer **7**, and thus we define a chemical shift for **5c** when it is hydrogen bonded in the cyclic trimer **7** ( $\delta_{5c}^7$ ). It can be assumed that the strength and the geometry of the different self-associations of **5** (from **5t** or **5c**) are similar and occur with the same association constant; resulting in that **5** gives rise to the same chemical shift when it is hydrogen bonded in a chain, no matter if the association involves **5c** or **5t**. A similar assumption is made for the association of **4** to **5** in a

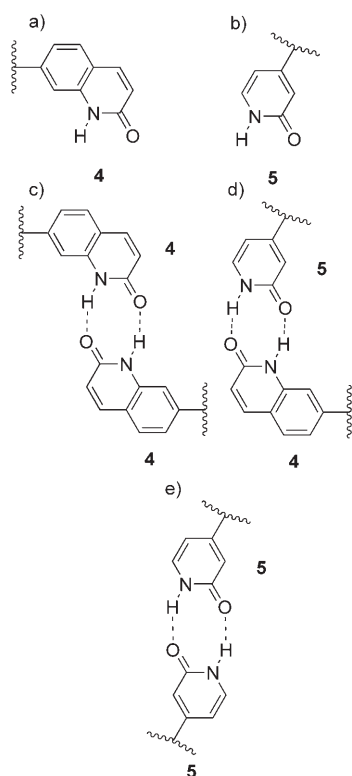


Figure 8. The definition of the chemical shift of the NH proton resonance of the 2-pyridone moiety in different states: a) **4** unbound ( $\delta_4^{\text{free}}$ ); b) **5** unbound ( $\delta_5^{\text{free}}$ ); c) **4** hydrogen bonded to **4** in polymer ( $\delta_4^{\text{44}}$ ); d) **4** hydrogen bonded to **5** in polymer ( $\delta_4^{\text{45}}$ ); in heterodimer **6** ( $\delta_4^{\text{6}}$ ); **5** hydrogen bonded to **4** in polymer ( $\delta_5^{\text{45}}$ ); in heterodimer **6** ( $\delta_5^{\text{6}}$ ); e) **5** hydrogen bonded to **5** in polymer ( $\delta_5^{\text{55}}$ ); **5c** hydrogen bonded to **5c** in cyclic trimer **7** ( $\delta_{5c}^{\text{7}}$ ).

chain. On the other hand, when **5c** is hydrogen bonded to **4** in the heterodimer **6** or the cyclic trimer **7**, the strength and geometry is most probably different, and thus the chemical shifts for the 2-pyridone/2-quinolone NH proton resonances of **5c** and **4** were assumed to be different.

*Estimation of the thermodynamic parameters and corresponding equilibrium constants for the case study (system 4+5) using NMR dilution titrations:* Three different experiments were carried out, each at five to six different temperatures in the range 233–313 K. Two in which salen **4** and porphyrin **5** were used separately in NMR dilution titration experiments: the NH proton resonance in the 2-pyridone/2-quinolone motif was monitored as the total concentration of monomers was altered systematically for **4** and **5**, respectively, and a third one in which a mixture of **4** and **5** in equimolar ratio was investigated in the same way. The first two experiments were used to obtain an initial estimate of the self-association constants ( $K_{44}$  for **4** and  $K_{55}$  for **5**) as well as the equilibrium constant for the isomerization of **5** ( $K_i$ ) and for the formation of cyclic trimer **7** from a linear trimer of **5c** ( $K_7$ ) (see Supporting Information for details). The third one was used to obtain an initial estimate of the association constant for the formation of cyclic dimer **6** from the linear dimer **4<sub>1</sub>5c<sub>1</sub>** ( $K_6$ ) and of the hetero-association constant  $K_{45}$ .

Finally, the observed proton resonances from all three dilution titration experiments were used together to obtain a globally better estimate of all the above-mentioned equilibrium constants. The concentrations in the titration span 0.30 to 30 mM. The lower part of the interval was set by the extended broadness of the observed 2-pyridone proton resonance and the higher by the limited solubility of the components in  $\text{CDCl}_3$ .

*NMR dilution titration experiments using 4:* In this system there is only one monomer **4**, as seen from the NMR spectra in Figure 6 (top), and therefore the different equations are reduced to the EK model and the different matrices are  $\Delta_c = (c_4)$  and  $\mathbf{K} = (K_{44})$ . The total concentration of monomer is computed by using Equation (10), which then reduces to Equation (44).

$$T_4 = \frac{c_4}{(1 - K_{44}c_4)^2} \quad (44)$$

From Equation (39), the chemical shifts of **4** can be computed [Eq. (45)].

$$\delta_4 = \frac{1}{(1 - K_{44}c_4)T_4} \delta_4^{\text{free sites}} + \frac{K_{44}c_4}{(1 - K_{44}c_4)^2 T_4} \delta_4^{\text{44}} \quad (45)$$

*NMR dilution titration experiments using 5:* This system is a bit more complicated since there are two monomers, **5t** and **5c** as seen from the NMR spectra in Figure 6 (middle), interconverting in the isomerization equilibrium [Eq. (43)]. However, there is only one association constant for the elongation of the supramolecular polymer, since it is assumed that it occurs with the same association constant for **5c** or **5t** [ $K_{5c5c} = K_{5t5t} = K_{5c5t} = K_{55}$ , Eq. (40)]. Furthermore, there are two additional equilibrium constants, the formation of the cyclic trimer **7** and the isomerization of **5**, respectively  $K_7$  [Eq. (42)] and  $K_i$  [Eq. (43)].

The mass balance for **5** can be decomposed into two different terms [Eq. (46)], in which  $T_{5t}$  and  $T_{5c}$  represent the total concentration of respectively **5t** and **5c** in any forms (in polymers for **5c** and **5t**, in cyclic trimer **7** for **5c** and as unbound).

$$T_5 = T_{5t} + T_{5c} \quad (46)$$

From Equation (10) we can get Equation (47) to compute the total concentration for **5t** and the total concentration of **5c** is computed [Eq. 48] from a combination of Equations (10), (40), and (42).

$$T_{5t} = c_{5t}^{-1} (\mathbf{1}^T (\Delta_c^{-1} - \mathbf{K})^{-1} \mathbf{1}_{5t})^2 \quad (47)$$

$$T_{5c} = c_{5c}^{-1} (\mathbf{1}^T (\Delta_c^{-1} - \mathbf{K})^{-1} \mathbf{1}_{5c})^2 + 3 K_{55}^2 K_7 c_{5c}^3 \quad (48)$$

$$\text{with } \Delta_c = \begin{pmatrix} c_{5t} & 0 \\ 0 & c_{5c} \end{pmatrix} \text{ and } \mathbf{K} = \begin{pmatrix} K_{55} & K_{55} \\ K_{55} & K_{55} \end{pmatrix}.$$

Using matrix algebra, Equations (47) and (48) can be reduced to Equations (49) and (50).

$$T_{5t} = \frac{c_{5t}}{(1 - K_{55}(c_{5t} + c_{5c}))^2} \quad (49)$$

$$T_{5c} = \frac{c_{5c}}{(1 - K_{55}(c_{5t} + c_{5c}))^2} + 3K_{55}^2 K_7 c_{5c}^3 \quad (50)$$

Finally, by summing up Equations (49) and (50) as stated in Equation (46), we can compute the total concentration of **5** as Equation (51).

$$T_5 = \frac{c_{5t} + c_{5c}}{(1 - K_{55}(c_{5t} + c_{5c}))^2} + 3K_{55}^2 K_7 c_{5c}^3 \quad (51)$$

Using Equation (39) and the matrices as defined above, the chemical shifts for **5t** and **5c** can be computed from Equations (52) and (53), respectively.

$$\delta_{5t} = \frac{c_{5t}}{(1 - K_{55}(c_{5t} + c_{5c}))T_{5t}} \delta_5^{\text{free}} + \frac{(c_{5t} + c_{5c})K_{55}c_{5t}}{(1 - K_{55}(c_{5t} + c_{5c}))^2 T_{5t}} \delta_5^{55} \quad (52)$$

$$\delta_{5c} = \frac{c_{5c}}{(1 - K_{55}(c_{5t} + c_{5c}))T_{5c}} \delta_5^{\text{free}} + \frac{(c_{5t} + c_{5c})K_{55}c_{5c}}{(1 - K_{55}(c_{5t} + c_{5c}))^2 T_{5c}} \delta_5^{55} + \frac{3K_{55}^2 K_7 c_{5c}^3}{T_{5c}} \delta_{5c}^7 \quad (53)$$

*NMR dilution titration experiments using 4+5:* Here we have three different monomers, **4**, **5c**, and **5t**, as seen in the NMR spectra in Figure 6 (bottom), and two additional association constants: the formation of the heterodimer **6** from a linear dimer composed of **4** and **5c**,  $K_6$  [Eq. (41)], and the elongation of the supramolecular polymer,  $K_{45}$ , in which **4** associates with **5** and vice versa.

The matrices for the polymeric part of the system **4+5** are

$$\Delta_c = \begin{pmatrix} c_{5t} & 0 & 0 \\ 0 & c_{5c} & 0 \\ 0 & 0 & c_4 \end{pmatrix} \text{ and}$$

$$K = \begin{pmatrix} K_{55} & K_{55} & K_{45} \\ K_{55} & K_{55} & K_{45} \\ K_{45} & K_{45} & K_{44} \end{pmatrix}.$$

The mass balances for **4**, **5c**, and **5t** can be computed from Equations (10), (41), and (42) as Equations (54)–(56), and the total concentration of **5** is given by Equation (57).

$$T_4 = c_4^{-1}(\mathbf{1}^T(\Delta_c^{-1} - \mathbf{K})^{-1}\mathbf{1}_4)^2 + K_{45}K_6 c_4 c_{5c} \quad (54)$$

$$T_{5t} = c_{5t}^{-1}(\mathbf{1}^T(\Delta_c^{-1} - \mathbf{K})^{-1}\mathbf{1}_{5t})^2 \quad (55)$$

$$T_{5c} = c_{5c}^{-1}(\mathbf{1}^T(\Delta_c^{-1} - \mathbf{K})^{-1}\mathbf{1}_{5c})^2 + 3K_{55}^2 K_7 c_{5c}^3 + K_{45}K_6 c_4 c_{5c} \quad (56)$$

$$T_5 = c_{5t}^{-1}(\mathbf{1}^T(\Delta_c^{-1} - \mathbf{K})^{-1}\mathbf{1}_{5t})^2 + c_{5c}^{-1}(\mathbf{1}^T(\Delta_c^{-1} - \mathbf{K})^{-1}\mathbf{1}_{5c})^2 + 3K_{55}^2 K_7 c_{5c}^3 + K_{45}K_6 c_4 c_{5c} \quad (57)$$

Leading on Equation (39), the chemical shifts for **4**, **5t**, and **5c**, can be computed from Equations (58)–(60), remembering that each component contains two identical binding sites.

$$\delta_4 = \frac{2 \times \mathbf{1}^T(\Delta_c^{-1} - \mathbf{K})^{-1}\mathbf{1}_4}{2T_4} \delta_4^{\text{free}} + \frac{2 \times \mathbf{1}^T(\Delta_c^{-1} - \mathbf{K})^{-1}\mathbf{1}_4 K_{44} \mathbf{1}_4^T(\Delta_c^{-1} - \mathbf{K})^{-1}\mathbf{1}}{2T_4} \delta_4^{44} + \frac{2 \times \mathbf{1}^T(\Delta_c^{-1} - \mathbf{K})^{-1}(\mathbf{1}_4 K_{45} \mathbf{1}_{5t}^T + \mathbf{1}_4 K_{45} \mathbf{1}_{5c}^T)(\Delta_c^{-1} - \mathbf{K})^{-1}\mathbf{1}}{2T_4} \delta_4^{45} + \frac{2K_{45}K_6 c_4 c_{5c}}{2T_4} \delta_4^6 \quad (58)$$

$$\delta_{5t} = \frac{2 \times \mathbf{1}^T(\Delta_c^{-1} - \mathbf{K})^{-1}\mathbf{1}_{5t}}{2T_{5t}} \delta_{5t}^{\text{free}} + \frac{2 \times \mathbf{1}^T(\Delta_c^{-1} - \mathbf{K})^{-1}(\mathbf{1}_{5t} K_{55} \mathbf{1}_{5t}^T + \mathbf{1}_{5t} K_{55} \mathbf{1}_{5c}^T)(\Delta_c^{-1} - \mathbf{K})^{-1}\mathbf{1}}{2T_{5t}} \delta_5^{55} + \frac{2 \times \mathbf{1}^T(\Delta_c^{-1} - \mathbf{K})^{-1}\mathbf{1}_{5t} K_{45} \mathbf{1}_4^T(\Delta_c^{-1} - \mathbf{K})^{-1}\mathbf{1}}{2T_{5t}} \delta_5^{45} \quad (59)$$

$$\delta_{5c} = \frac{2 \times \mathbf{1}^T(\Delta_c^{-1} - \mathbf{K})^{-1}\mathbf{1}_{5c}}{2T_{5c}} \delta_{5c}^{\text{free}} + \frac{2 \times \mathbf{1}^T(\Delta_c^{-1} - \mathbf{K})^{-1}(\mathbf{1}_{5c} K_{55} \mathbf{1}_{5t}^T + \mathbf{1}_{5c} K_{55} \mathbf{1}_{5c}^T)(\Delta_c^{-1} - \mathbf{K})^{-1}\mathbf{1}}{2T_{5c}} \delta_5^{55} + \frac{2 \times \mathbf{1}^T(\Delta_c^{-1} - \mathbf{K})^{-1}\mathbf{1}_{5c} K_{45} \mathbf{1}_4^T(\Delta_c^{-1} - \mathbf{K})^{-1}\mathbf{1}}{2T_{5c}} \delta_5^{45} + \frac{2K_{55}^2 K_7 c_{5c}^3}{2T_{5c}} \delta_{5c}^7 + \frac{2K_{45}K_6 c_4 c_{5c}}{2T_{5c}} \delta_{5c}^6 \quad (60)$$

Since the isomerization process of **5** is slower than the NMR timescale, it is possible to know the ratio of the total concentration of **5c** and **5t** [ $R_{ct}$ , Eq. (61)].

$$R_{ct} = \frac{T_{5c}}{T_{5t}} \quad (61)$$

The experimental value is obtained by measuring the ratio of the integral of a specific proton resonance of **5** in **5c** and **5t** in the aromatic region. The peak giving the best base line separation was used.

*Estimation of the thermodynamic data and calculation of the equilibrium constants of the system 4+5:* Following the fitting procedure described in the Supporting Information, we obtained the thermodynamic data for the different equilibria representing the system **4+5** as defined in Equations (40)–(43). The results are summarized in Tables 1 and 2. The temperature span for which the change in standard entropy is recorded is only 53–83 °C due to the limited solubility of the

Table 1. Estimated thermodynamic parameters<sup>[a]</sup> for the different equilibria as defined in Equations (40)–(43) in CDCl<sub>3</sub> based on the fitting of the derived general mathematical EK model to the NMR dilution titration data.

Entry	Equilibrium	$\Delta H^\circ$ [kJ mol <sup>-1</sup> ]	$\Delta S^\circ$ [J mol <sup>-1</sup> K <sup>-1</sup> ]
1	$K_{55}$	$-32 \pm 3$	$-42 \pm 5$
2	$K_{44}$	$-29 \pm 1$	$-53 \pm 4$
3	$K_{45}$	$-18 \pm 5$	$-11 \pm 16$
4	$K_6$	$-24 \pm 5$	$-57 \pm 16$
5	$K_7$	$-15 \pm 4$	$-26 \pm 13$
6	$K_i$	$-5 \pm 4$	$-16 \pm 12$

[a] 95% confidence interval.

Table 2. Estimated chemical shifts<sup>[a]</sup> of the proton resonances of the different hydrogen-bonding NH 2-pyridone motifs in CDCl<sub>3</sub> for the different states of system **4+5** as defined in Figure 8 based on the fitting of the derived general mathematical EK model to the NMR dilution titration data.

Entry	Hydrogen-bonding motif	Chemical shift [ppm]
1	$\delta_4^{\text{free}}$	$8.56 \pm 0.06$
2	$\delta_4^{44}$	$13.14 \pm 0.08$
3	$\delta_4^{45}$	$13.53 \pm 0.32$
4	$\delta_4^6$	$13.81 \pm 0.58$
5	$\delta_5^{\text{free}}$	$8.80 \pm 0.14$
6	$\delta_5^{55}$	$14.14 \pm 0.02$
7	$\delta_5^{45}$	$13.98 \pm 0.18$
8	$\delta_{5c}^6$	$14.18 \pm 0.12$
9	$\delta_{5c}^7$	$14.55 \pm 0.14$

[a] 95% confidence interval.

components, and therefore these data are less accurate compared to the standard enthalpy data. The quality of the fit is demonstrated in Figures 9 and 10. Figure 9 shows as examples the systems **4**, **5**, and **4+5** at one of the investigated temperatures (283–284 K); the observed chemical shifts of the three observed NH 2-pyridone/2-quinolone protons, NH<sub>4</sub>, NH<sub>5c</sub> and NH<sub>5t</sub> are plotted for each concentration investigated together with the best fit of the derived complete mathematical association model to these data. During the dilution titrations at 283–284 K, the degree of association varies from 6 to 99% for **4** in system **4**, from 55 to 100% for **5** in system **5**, and finally from 34 to 95% for **4** and 67 to 99% for **5** in system **4+5**. Apart from the titration of system **4**, the two other titrations are not completely in the optimum interval for NMR titrations (roughly speaking the degree of association should be from 20 to 80%<sup>[32]</sup>), due to constraints in the sensitivity of the NMR signal and the limited solubility of the components. However, the high number of data points used in the final fitting (approximately, 300) including many systems, **4**, **5**, and **4+5**, studied over many different temperatures, is expected to compensate for the above-mentioned shortcoming, leading to high accuracy of the model, supported by the fact that the obtained values of  $\Delta H^\circ$  for the different 2-pyridone/2-quinolone binding motifs in system **4+5** correlates within the 95% confidence interval with the reported value for the dimerization of 2-pyridone itself (vide infra). Moreover, as can be seen in Figure 10a–c,

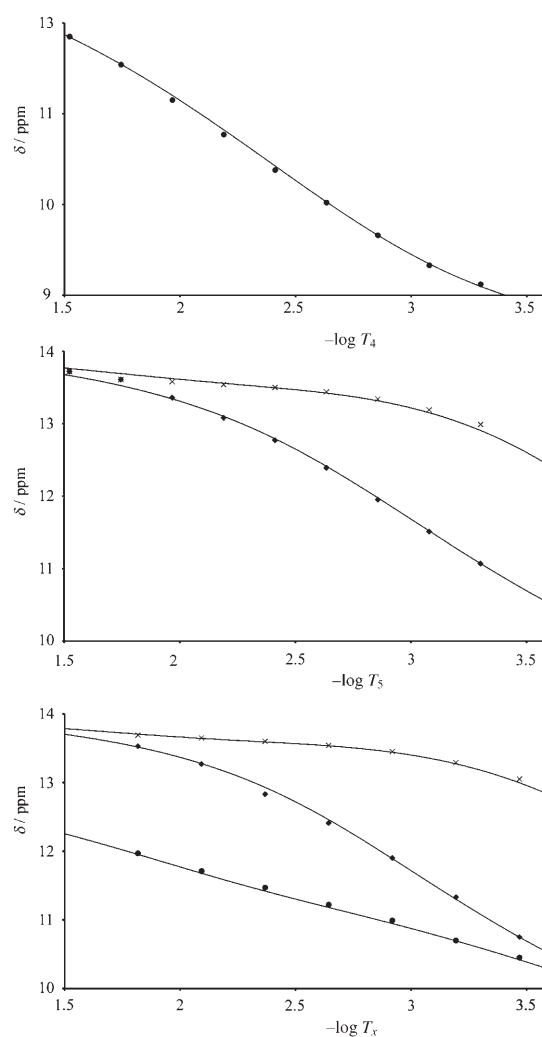


Figure 9. Observed chemical shifts of the NH proton resonances of the 2-pyridone (2-quinolone) moieties (● for **4**, ◆ for **5t** and × for **5c**) in the different NMR dilution titrations at 283–284 K in CDCl<sub>3</sub>. The solid line represents the best fit of the derived general mathematical EK model to the experimental data. Top: Titration of **4**. Middle: Titration of **5**. Bottom: Titration of system **4+5** (1:1) and  $T_x = T_4 = T_5$ .

the observed and calculated shifts for the three NH-proton resonances of the 2-pyridone/2-quinolone moieties correlate well over the investigated concentration ranges. The observed shifts as seen in Figure 10a–c were measured with high accuracy from the NMR spectra; however, the  $R_{ct}$  values that were obtained from the ratio of the same proton resonance, one from the *cisoid* and one from the *transoid* compound, **5c** and **5t**, respectively, in separate experiments at different temperatures and concentrations, were not as accurate since the signals were sometimes overlapping. However, the  $R_{ct}$  values were needed to constrain the model and since the expression for the  $R_{ct}$  is not a linear combination of independent variables (as is the case for the chemical shift), the model cannot be adjusted to give a better fit, thus the worse correlation between observed and calculated data in Figure 10d compared to Figure 10a–c.

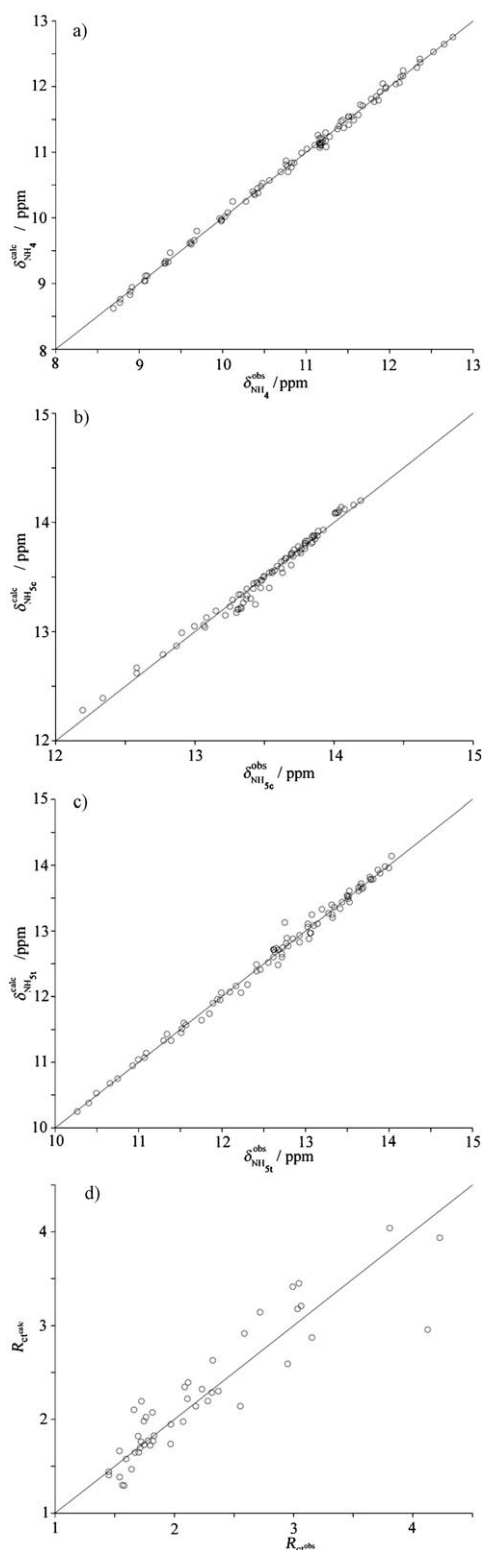


Figure 10. Correlation between calculated and observed chemical shifts and  $R_{ct}$  values for system **4+5** in  $CDCl_3$  for the final fitting of the derived general mathematical EK model to the data from the NMR dilution titrations: a) NH proton resonances of the 2-pyridone (2-quinolone) motif in **4**. b) NH proton resonances of the 2-pyridone moiety in **5c**. c) NH proton resonances of the 2-pyridone moiety in **5t**. d)  $R_{ct}$  values for **5**.

The excellent correlations in Figures 9 and 10 support the EK model for the formation of the different aggregates in the system **4+5**.

As can be seen in Table 1, the homo-association of respective components **4** and **5** to linear structures is the most stable type of association (entries 1 and 2,  $\Delta H^\circ$ ), except for the formation of the cyclic structure **7** (entry 5,  $\Delta H^\circ$ ). However, hetero-association of **4** and **5** forming linear structures (entry 3,  $\Delta H^\circ$ ) is less stable and the value of  $\Delta H^\circ$  deviates to some extent from the one for 2-pyridone itself, whereas the hetero-associations forming the cyclic structures **6** correlate well with the latter (entry 4,  $\Delta H^\circ$ ). It can be anticipated that the homo-association of such systems based on the 2-pyridone hydrogen-bonding motif should be more stable than for the corresponding hetero-associated systems due to a perfect match between the two (identical) hydrogen bonds involved in the former case, compared to the hetero-associated system in which, for example, one of the two hydrogen bonds (not identical) could be a little bit longer than the other, making the second a somewhat weaker.

It is notable that the change in standard enthalpy ( $\Delta H^\circ$ ) for all the associations involving structures based on the 2-pyridone hydrogen-bonding pattern, represented by the equilibria in Equation (40) ( $K_{44}$ ,  $K_{55}$ ,  $K_{45}$ ) is close to the reported value for the dimerization of 2-pyridone itself in  $CHCl_3$ ,  $\Delta H^\circ = -25.3 \text{ kJ mol}^{-1}$  when taking into account the 95% confidence intervals of the former.<sup>[19]</sup> Importantly, this similarity provides a positive validation of the extended equal  $K$  model derived in this study.

Another observation is that the loss in standard entropy for the formation of a homodimer of **4** is more pronounced than for **5** (entries 1 and 2,  $\Delta S^\circ$ ). This difference in the change of entropy for the formation of a homodimer of either **4** or **5** induces a large difference in the corresponding self-association constants (Tables 3 and 4), as calculated

Table 3. Estimated association constants<sup>[a,b]</sup> as defined in Equation (40) (oligomerizations) at the different temperatures used in the NMR dilution titration experiments in  $CDCl_3$ .

Entry	$T$ [K]	$10^{-2} \cdot K_{44}$ [ $M^{-1}$ ]	$10^{-3} \cdot K_{55}$ [ $M^{-1}$ ]	$10^{-2} \cdot K_{45}$ [ $M^{-1}$ ]
1	233	45 (38, 52)	78 (67, 91)	26 (13, 50)
2	263	8.2 (7.3, 9.1)	12 (11, 14)	9.0 (6.1, 14)
3	273	5.0 (4.5, 5.6)	7.1 (6.5, 7.8)	6.7 (4.8, 9.3)
4	283	3.2 (2.9, 3.6)	4.3 (4.0, 4.8)	5.1 (3.8, 6.7)
5	298	1.7 (1.5, 1.9)	2.2 (2.0, 2.4)	3.5 (2.7, 4.4)
6	312	0.99 (0.91, 1.1)	1.2 (1.0, 1.4)	2.5 (1.9, 3.1)

[a] 95% confidence interval (min, max). [b] The estimated association constants are based on the fitting of the derived general mathematical EK model to the NMR dilution titration data.

from the thermodynamic parameters at the temperatures used in the NMR dilution titrations.

In the equal  $K$  model all association constants between the same type of binding elements are the same independent of where in an assembly they might appear. Including the possibility of cooperative effects in the association to linear copolymers would necessarily mean that  $K_n \neq K_{n+1}$  thus increasing the number of parameters to be included in

Table 4. Estimated association constants<sup>[a,b]</sup> as defined in Equations (41)–(43) (cyclizations and isomerization) at the different temperatures used in the NMR dilution titration experiments in CDCl<sub>3</sub>.

Entry	<i>T</i> [K]	10 <sup>-1</sup> · <i>K</i> <sub>6</sub> [M <sup>-1</sup> ]	<i>K</i> <sub>7</sub> [M <sup>-2</sup> ]	<i>K</i> <sub>i</sub>
1	233	25 (15, 41)	92 (57, 150)	1.7 (1.2, 2.4)
2	263	6.0 (4.6, 7.8)	38 (29, 50)	1.3 (1.1, 1.5)
3	273	4.0 (3.2, 5.0)	30 (24, 37)	1.2 (1.0, 1.3)
4	283	2.8 (2.3, 3.3)	24 (19, 28)	1.1 (1.0, 1.2)
5	298	1.6 (1.3, 2.0)	17 (14, 20)	1.0 (0.92, 1.1)
6	312	1.0 (0.84, 1.3)	13 (10, 16)	0.91 (0.70, 1.1)

[a] 95% confidence interval (min, max). [b] The estimated association constants are based on the fitting of the derived general mathematical EK model to the NMR dilution titration data.

the fitting compared to the present mathematical model.<sup>[33]</sup> The fact that the fitting of the extended equal *K* model to the experimental data for the system is excellent as seen in Figures 9 and 10, indicates that the system is non-cooperative. Moreover, it could have been speculated that such mechanism would have been likely due to the possibility to form π–π interactions between different turns of the linear supramolecular oligomers in the system **4+5**, if the oligomers would exist in helical conformations. However, the chemical shifts of the proton resonances of the aromatic structural units in system **4+5** are very little affected by change in the total concentration of the system, indicating the lack of π–π interactions and thereby making the formation of tight helical conformations and thus cooperative mechanisms for the association of the monomers, less likely. This view is also supported by the fact that the distance between the two binding sites of each monomer **4** and **5**, respectively, is relatively large; in addition, the connection between them is flexible making one predominant conformation, advantageous for helical cooperative binding, less likely.

As expected, the formation of the cyclic heterodimer **6** from the linear dimer **4,5c**<sub>1</sub> is very much disfavored by entropy compared to the formation of **4,5c**<sub>1</sub>, Δ*S*<sup>o</sup> = –57.2 and –11.3 J mol<sup>-1</sup> K<sup>-1</sup>, respectively (Table 1, entries 3 and 4). This is due to the extensive loss of degrees of freedom of the components **4** and **5c** upon formation of **6** compared to what it is the case upon formation of **4,5c**<sub>1</sub> from the respective monomers. The formation of **6** from **4,5c**<sub>1</sub> is only slightly favored by enthalpy compared the formation of **4,5c**<sub>1</sub> from **4** and **5c**, Δ*H*<sup>o</sup> = –24 and –18 kJ mol<sup>-1</sup>, respectively (Table 1, entries 3 and 4). These results can be explained by the fact that the angle between the two aromatic planes of the 2-pyridone - aryl system of **5c** must have a value close to zero, causing steric strain, to obtain a good planarity of the hydrogen bond between the 2-quinolone of **4** and the 2-pyridone of **5c** to form **6**.

On the other hand, the formation of the cyclic trimer **7** is disfavored by enthalpy and favored by entropy, if we compare the enthalpy and entropy of formation of a linear trimer **5c**<sub>3</sub> and the one for the formation of **7** from **5c**<sub>3</sub> (Table 1, entries 1 and 5).

*Determination of some of the different parameters characterizing system 4+5:* The different association and equilibrium

constants for the system **4+5** can be used to calculate the different parameters characteristic of the supramolecular system. Such parameters include the degree of polymerization, the mole fractions of a given monomer in different aggregates, macrocycle and oligomers, present in the solution at different concentrations of the monomers and the mole fraction of a given monomer at a given position in oligomers, using the expressions derived for the general association model (vide supra).

*The average degree of polymerization:* By using Equation (12), the degree of polymerization (DP) of the system **4+5** was investigated within the solubility range in CDCl<sub>3</sub> at 298 K (Figure 11). First it should be noted that the values of

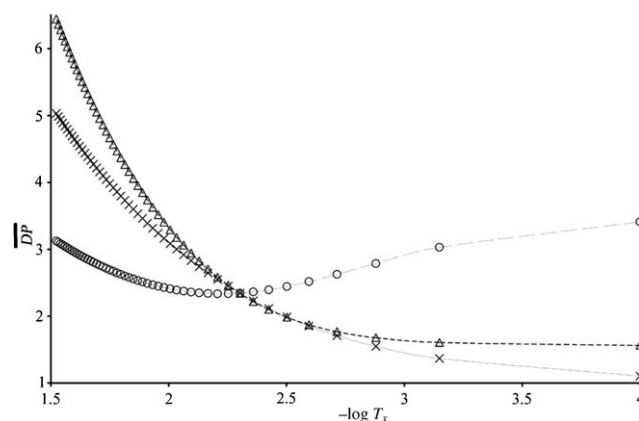


Figure 11. The average degree of polymerization at different concentration of salen **4** and porphyrin **5** in CDCl<sub>3</sub> at 298 K. *T*<sub>4</sub> = 5.0 mM and *T*<sub>5</sub> varies (△), *T*<sub>5</sub> = 5.0 mM and *T*<sub>4</sub> varies (○) and *T*<sub>x</sub> = *T*<sub>4</sub> = *T*<sub>5</sub> (×).

DP are low, indicating the formation of oligomers instead of polymers. Moreover, as can be seen from Figure 11 (△), DP is strongly influenced by the addition of **5** to a 5.0 mM solution of **4**. The DP value changes from 1.5 before the addition, to 6.4, when 6 equivalents of **5** have been added (*T*<sub>5</sub> = 30 mM, –log *T*<sub>5</sub> = 1.52). On the other hand, the addition of **4** to a 5.0 mM solution of **5** decreases the DP until the total concentration of **4** passes 6.8 mM. At higher concentrations the DP starts to increase again (Figure 11, ○). Finally, the DP is equal to 2.3 when *T*<sub>4</sub> = *T*<sub>5</sub> = 5.0 mM and reaches a maximum of **5** at 30 mM (–log *T*<sub>5</sub> = 1.52) (Figure 11, ×), the highest possible concentration due to the limited solubility of **5** in CDCl<sub>3</sub>.

*The distribution of monomer 4 and 5 (2 and 3) among different species in system 4+5 (2+3):* From Equations (14) and (18), the distribution of one particular monomer among different oligomers (polymers) at a given concentration of monomers within the solubility range of the system **4+5** in CDCl<sub>3</sub> at 298 K can be calculated. From Equation (14) (in which the index “polymer” is exchanged for one of the macrocyclic species **6** and **7**) and Equations (40)–(42) the distribution of **4** and **5** in cyclic species can be computed with

Equations (62)–(64). Finally the mole fractions of **4** and **5** as unbound species are given by Equations (65) and (66).

$$\chi_4^6 = \frac{K_{45}K_6c_4c_5c}{T_4} \quad (62)$$

$$\chi_5^6 = \frac{K_{45}K_6c_4c_5c}{T_5} \quad (63)$$

$$\chi_5^7 = \frac{3K_{55}^2c_5^3c}{T_5} \quad (64)$$

$$\chi_4^{\text{free}} = \frac{c_4}{T_4} \quad (65)$$

$$\chi_5^{\text{free}} = \frac{c_5}{T_5} \quad (66)$$

Figure 12 shows the mole fractions of **5** bound as oligomers, as macrocycles **6** and **7**, and as unbound monomers at different concentrations of monomers **4** and **5**. As can be seen, the addition of salen **4** to a solution of porphyrin **5** in CDCl<sub>3</sub> (5.0 mM) does not have any effect on the mole fraction of **5** involved in oligomers or as unbound; however, the mole fraction of **5** bound as cyclic trimer **7** or cyclic heterodimer **6** varies (Figure 12a,  $\diamond$  and  $\blacklozenge$  respectively). At concentrations higher than 2.45 mM ( $-\log T_4=2.61$ ), salen **5** is bound in **6** to a larger extent than in **7**. On the other hand, addition of **5** to a solution of **4** in CDCl<sub>3</sub> (5.0 mM) results in a different case (Figure 12b). Now, the predominant form of **5** is as a part of **6** at low concentrations of **5**. At concentrations of **5** higher than 1 mM ( $-\log T_5=3$ ), monomer **5** as a part of oligomers predominates. At concentration of **5** higher than 11 mM ( $-\log T_5=1.96$ ) the mole fraction of **5** bound as **7** is higher than bound as **6**, but still lower than that bound as oligomers (Figure 12b). When the concentration of **5** is varied in the absence of **4**, the predominant form of **5** is as unbound monomer, and at high concentrations it is dominant as a part of oligomers, as one would expect from supramolecular polymers (oligomers) (Figure 12c). The mole fraction of **5** bound as **7** has its maximum at a concentration of 1.3 mM ( $-\log T_5=2.89$ ) but still never being the predominant species in solution. In a 1:1 mixture of **4** and **5**, the predominant form of **5** is as monomer at low concentration and as part of oligomers at high concentration (Figure 12d). Having **5** bound as **6** is always more predominant than having it bound as **7**.

The analysis above can also be carried out for the monomer **4**; however, from now on we will refer to the actual catalyst **2** instead (and also receptor **3** instead of the corresponding model **5**), since those mole fractions are of interest for an elaborate investigation of the substrate selectivity observed in the epoxidations of olefinic substrates using system **2+3**.<sup>[18]</sup> This allows us to demonstrate the importance of being able to characterize weak dynamic supramolecular systems and in this specific case the catalytic properties of the system, something that is now achievable by the derived methodology in the present paper, but the details are dis-

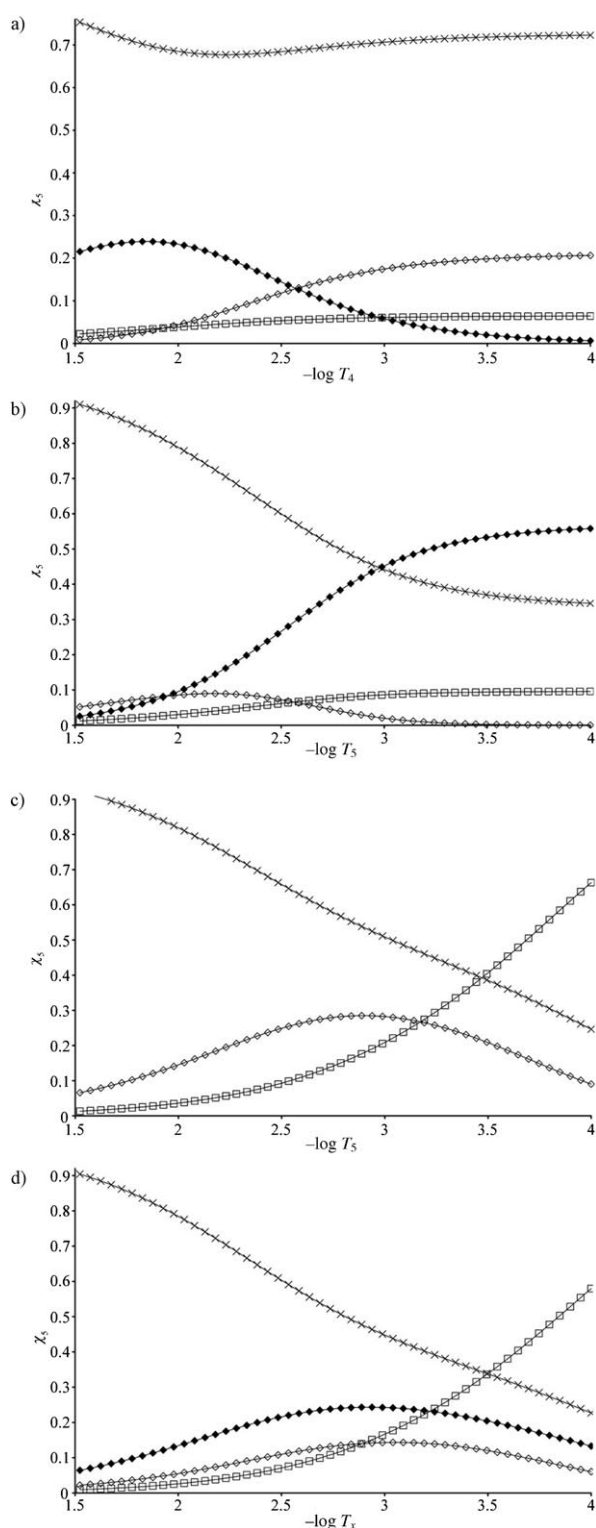


Figure 12. Calculated variations of the mole fraction of porphyrin **5** in different species  $\chi_5^x$  at different concentrations of **4** and **5** in CDCl<sub>3</sub> at 298 K: unbound,  $\chi_5^{\text{free}}$  ( $\square$ ), in oligomers **4<sub>n</sub>5<sub>m</sub>**,  $\chi_5^{\text{oligomers}}$  ( $\times$ ), in cyclic heterodimer **6**,  $\chi_5^6$  ( $\blacklozenge$ ), in cyclic trimer **7**,  $\chi_5^7$  ( $\diamond$ ). a)  $T_4$  varies and  $T_5=5.0$  mM. b)  $T_5$  varies and  $T_4=5.0$  mM. c)  $T_5$  varies and  $T_4=0$  mM. d) Dilution of a 1:1 mixture of **4** and **5**.



cussed elsewhere.<sup>[18]</sup> The derivation of the model in the present paper was primarily done to further analyze the system **2+3** in the selective catalytic epoxidation of pyridine-appended olefins over phenyl-appended ones. In our preliminary studies it was concluded that heterodimer **1** represented more than 70% of all the species in solution.<sup>[18a]</sup> This value was obtained from a simplified model neglecting the oligomers of any type fitted to the observed substrate selectivity at different total concentrations of **2** and **3** in competitive epoxidations.<sup>[18a]</sup> However, if we now assume that the metal-free system **4+5**, as analyzed in the present paper, represents the catalytic system **2+3**, the mole fraction of catalyst **2** bound in heterodimer **1**,  $\chi_2^1$ , represented by the mole fraction of **4** bound in **6**,  $\chi_4^6$ , [Eq. (62)] never exceeds 0.3. Notably this maximum is obtained already at low concentrations of **2** when the total concentration of **3** ( $T_3$ ) is 1.0 mM ( $-\log T_3=3$ ) (Figure 13a, ●). In fact, the mole fraction of **2** bound as **1** over the range of concentrations used during the investigation of substrate selectivity of system **2+3**<sup>[18b]</sup> was rather constant, never exceeding 0.2 (Table 5). Therefore

Table 5. Calculated mole fraction of salen **2** as unbound species,  $\chi_2^{\text{free}}$ , as well as in cyclic heterodimer **1**,  $\chi_2^1$  at three different concentrations of **2** and **3** used in the catalytic competitive epoxidations,<sup>[18b]</sup> using the equilibrium data for the model **4+5** in  $\text{CDCl}_3$  at 298 K (estimated value  $\pm$  standard error).

Entry	$T_2$ [mM]	$T_3$ [mM]	$\chi_2^{\text{free[a]}}$	$\chi_2^{\text{1[b]}}$
1	5.0	5.0	$0.27 \pm 0.01$	$0.19 \pm 0.01$
2	5.0	15	$0.19 \pm 0.01$	$0.18 \pm 0.01$
3	0.50	0.50	$0.61 \pm 0.01$	$0.22 \pm 0.01$

[a] From Equation (65) setting  $\chi_2^{\text{free}} = \chi_4^{\text{free}}$ . [b] From Equation (62) setting  $\chi_2^1 = \chi_4^6$ .

the observed different substrate selectivities as a function of the concentrations of **2** and **3** in the competitive epoxidation are most probably not only explained by the presence of **1**.<sup>[18]</sup> In fact the only parameter that does vary at different concentrations is the mole fraction of **2** bound as co-oligomers and this should accordingly also account for the observed variation in substrate selectivity with concentration.

*Mole fraction of **2** (**4**) given in a specific environment of next-neighbors **2** or **3** (**4** or **5**) in the system **2+3** (**4+5**):* The calculation of the mole fraction in a specific environment is of more importance for the catalytic unit in the supramolecular oligomer, therefore they are only calculated for monomer **2** using **4** as a model for the actual system.

From Equations (26), (30), and (31), respectively, and assuming that the system **4+5** represents the actual catalytic system **2+3**, we can obtain the mole fraction of **2** adjacent to the same type of monomer (**2**;  $\chi_2^{(1)}$ ) to at least one monomer of different type (**3**;  $\chi_2^{(2)}$ ) and to exactly two monomers of different type (**3**;  $\chi_2^{(3)}$ ), in the system **2+3** (**4+5**) in total. The two last cases are calculated considering **3** (**5**) as one type of monomer. The results are presented in Figure 13 and in Table 5, also including the mole fraction of **2** as unbound and bound in **1**,  $\chi_2^{\text{free}}$  and  $\chi_2^1$ , respectively [Eqs. (65)

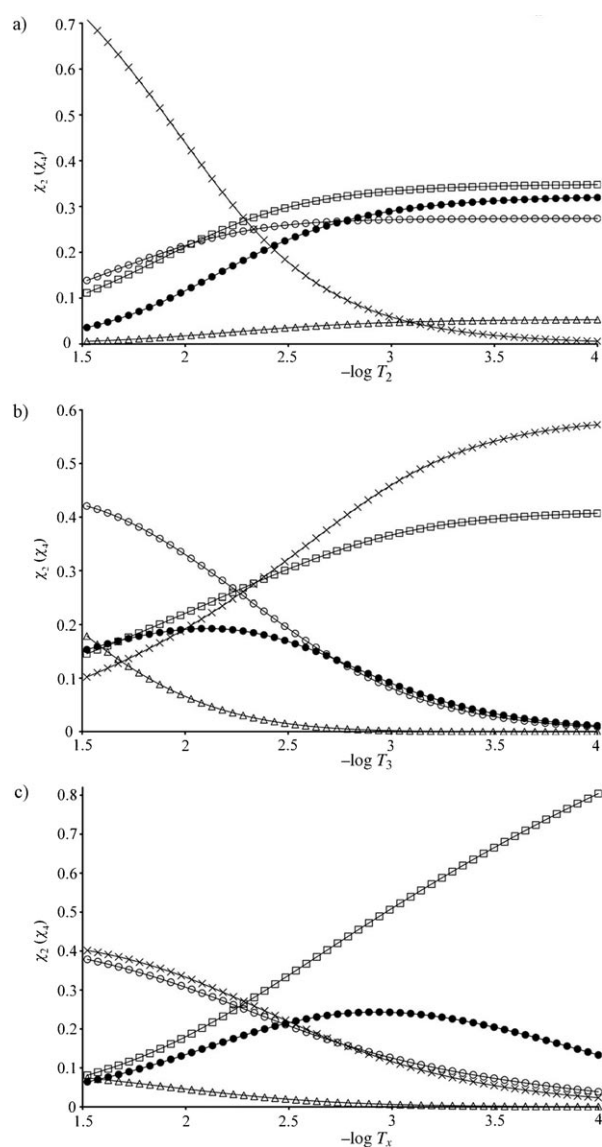


Figure 13. Calculated variations of the mole fraction of salen **2** (**4**) with concentrations, as unbound species,  $\chi_2^{\text{free}}$  ( $\square$ ), and in the cyclic heterodimer **1** (**6**),  $\chi_2^1$  ( $\bullet$ ), adjacent to another **2** (**4**),  $\chi_2^{(1)}$  ( $\times$ ), adjacent to exactly one porphyrin **3** (**5**),  $\chi_2^{(2)}$  ( $\circ$ ), and adjacent to porphyrin **3** (**5**) in both ends,  $\chi_2^{(3)}$  ( $\blacktriangle$ ), the three last mole fractions as an average for all species in the system **2+3** (**4+5**) in  $\text{CDCl}_3$  at 298 K. a)  $T_2$  varies and  $T_3=5.0$  mM. b)  $T_3$  varies and  $T_2=5.0$  mM. c) Dilution of a 1:1 mixture of **2+3** (**4+5**).

and (62), respectively, setting  $\chi_2^{\text{free}} = \chi_4^{\text{free}}$  and  $\chi_2^1 = \chi_4^6$ . In Table 5, these mole fractions are presented for the specific concentrations used in the catalytic competitive epoxidations.<sup>[18b]</sup> The importance of considering **2** and **3** as next neighbors for the substrate selectivity in the competitive epoxidation with system **2+3** is elaborated elsewhere,<sup>[18b]</sup> however, in the present context, it is worth noting that oligomers having **2** and **3** as next neighbors do contribute to the substrate selectivity together with **1**.<sup>[18b]</sup> In fact as can be seen from Tables 5 and 6, ( $\chi_2^{(2)} + \chi_2^{(3)}$  compared to  $\chi_2^1$ ), catalyst **2** with at least one receptor molecule **3** adjacent in oligomers or with **2** as unbound species is more predominant than **2**

Table 6. Calculated mole fraction of salen **2** adjacent to another **2**,  $\chi_2^{(1)}$ , adjacent to exactly one porphyrin **3**,  $\chi_2^{(2)}$ , and adjacent to **3** in both ends,  $\chi_2^{(3)}$ , as an average for all species in the system **2+3**, at three different concentrations of **2** and **3** used in the catalytic competitive epoxidations<sup>[18b]</sup> using the equilibrium data from the model **4+5** in CDCl<sub>3</sub> at 298 K (estimated value  $\pm$  standard error).

Entry	$T_2$ [mM]	$T_3$ [mM]	$\chi_2^{(1)[a]}$	$\chi_2^{(2)[b]}$	$\chi_2^{(3)[c]}$
1	5.0	5.0	0.27 $\pm$ 0.01	0.25 $\pm$ 0.01	0.029 $\pm$ 0.002
2	5.0	15	0.15 $\pm$ 0.01	0.37 $\pm$ 0.01	0.099 $\pm$ 0.007
3	0.50	0.50	0.074 $\pm$ 0.01	0.090 $\pm$ 0.004	0.0030 $\pm$ 0.0003

[a] From Equation (26) setting  $\chi_2^{(1)} = \chi_4^{(1)}$ . [b] From Equation (30) setting  $\chi_2^{(2)} = \chi_4^{(2)}$ . [c] From Equation (31) setting  $\chi_2^{(3)} = \chi_4^{(3)}$ .

bound in **1**, making the oligomers in which **2** and **3** are next neighbors, and free **2**, as much catalytic species as the originally proposed cyclic heterodimer **1** in the system **2+3**.

## Conclusion

A general mathematical model that is an extension of the equal *K* (EK) model and allows for the determination of association constants for dynamic supramolecular systems such as supramolecular linear copolymers has been derived without having to recourse to extensive approximations. The only limitation is the restricted number of experimental data for the estimation of the association constants. To our knowledge, this is the most elaborate model for dynamic supramolecular systems including supramolecular copolymers so far. It enables derivation of true association constants between the different monomers and characterization of the so-formed aggregates such as oligo- and polymers with respect to the average degree of polymerization, the distribution of the monomers among the different associated species, and the position of a certain type of monomer in the polymer. There are no restrictions neither in terms of what type of ditopic monomers employed, nor in terms of what type of different equilibrium constants being involved.

We also report here on the detailed procedure to obtain accurate value from the fitting by developing an advanced procedure in which the calibration of the above mathematical model is done with care by using NMR dilution titrations (see Supporting Information). The different parameters that are involved for each monomer are first estimated separately and then in turn the hetero-association constants are estimated by using a system in which all monomers have an equal concentration. Finally all the parameters are refined by fitting the entire set of data points at all temperatures to obtain the  $\Delta H^\circ$  and  $\Delta S^\circ$  from which the association constant could be calculated. This leads to a globally better fit compared to assessing the thermodynamic parameters from a linear regression of the logarithm of the equilibrium constants obtained separately at each temperature. To our knowledge this is the first time that such an advanced fitting procedure for models to NMR titration data is reported in the literature.

In applying the mathematical model on the metal-free system **4+5**, in which each component contains two identical hydrogen-bonding motifs based on the 2-pyridone moiety, different for **4** and **5**, constituting formally a two-component (but in reality a three-component) system, we show that the developed model could easily be extended to include in addition to linear co-oligomers also cyclic structures making this mathematical model useful for application on dynamic supramolecular systems in general. The fact that the obtained values of  $\Delta H^\circ$  for the different 2-pyridone binding motifs in system **4+5** correlates within the 95 % confidence interval with the reported value for the dimerization of 2-pyridone itself, constitute a valuable verification of our mathematical model. In addition to obtaining the different thermodynamic parameters for system **4+5**, the different parameters that characterize the formed supramolecular oligomers could be explicitly calculated.

The original aim of the work was to present an extension of the equal *K* model to assess the different association constants and the distribution of species in the catalytic system **2+3** using system **4+5** as a model. This has enabled us to refute the earlier conclusion that cyclic heterodimer **1** is the major species in solution. Instead the situation in which catalyst **2** is adjacent to at least one receptor molecule **3** in supramolecular oligomers is more predominant.

Although the present model system **4+5** is not designed to form exclusively supramolecular copolymers due to its low degree of polymerization and conformational freedom of the monomers, it allows us to demonstrate the machinery of the derived mathematical expression for the characterization of such species. This fact has enabled us to demonstrate the extension of the derived mathematical model to dynamic supramolecular systems in general in which many types of species apart from copolymers do appear, as in the system **4+5**. The application of the derived mathematical model on the system **4+5** has also demonstrated that even if an optimal concentration range for obtaining association constants from the NMR titrations cannot be obtained due to solubility and sensitivity reasons, the use of a high number of data points obtained by titrations of the different components together as well as alone, at different temperatures, can compensate for these shortcomings.

Finally, although not new as such, it is important to note that the present methodology in which the inclusion of equilibria where predictable but non-identified species participate, such as the cyclic trimer **7**, in the fitting of the model to experimental data, is to date the only means to identify weakly associated assemblies, in a supramolecular system for which direct methods of analyses fail.

## Acknowledgements

We are grateful to Dr. Ola F. Wendt and Mr. Roger Johansson for their expert assistance with the NMR spectrometer and Prof. Lars-Ivar Elding for discussions. We thank the Swedish Research Council, the Crafoord Foundation, the Lars-Johan Hierta Foundation, the Magnus Bergvall

Foundation and the Royal Physiographic Society, Lund for financial support.

- [1] a) H.-J. Schneider, A. Yatsimirsky, *Principles and Methods in Supramolecular Chemistry*, Wiley, Chichester, UK, **2000**; b) C. R. Cantor, P. R. Schimmel, *Biophysical Chemistry, Part II: Techniques for the Study of Biological Structure and Function*, Freeman, San Francisco, USA, **1980**.
- [2] For examples of reviews see: a) J.-M. Lehn, *Supramolecular Chemistry—Concepts and Perspectives*, VCH, Weinheim, **1995**, Chapter 9; b) C. T. Imrie, *Trends Polym. Sci.* **1995**, *3*, 22–29; c) F. Zeng, S. C. Zimmermann, *Chem. Rev.* **1997**, *97*, 1681–1712; d) R. F. M. Lange, M. van Gurp, E. W. Meijer, *J. Polym. Sci. Part A* **1999**, *37*, 3657–3670; e) J. S. Moore, *Curr. Opin. Colloid Interface Sci.* **1999**, *4*, 108–116; f) R. P. Sijbesma, E. W. Meijer, *Curr. Opin. Colloid. Interf. Sci.* **1999**, *4*, 24–32; g) L. Brunsveld, B. J. B. Folmer, E. W. Meijer, R. P. Sijbesma, *Chem. Rev.* **2001**, *101*, 4071–4097; h) J.-M. Lehn, *Polym. Int.* **2002**, *51*, 825–839; i) J.-C. Dai, Z.-Y. Fu, X.-T. Wu, *Encycl. Nanosci. Nanotechnol.* **2004**, *10*, 247–266; j) A. Ciferri, *Supramolecular Polymers*, Taylor and Francis, Boca Raton, USA, **2005**.
- [3] C. Fouquey, J.-M. Lehn, A.-M. Levelut, *Adv. Mater.* **1990**, *2*, 254–257.
- [4] For reviews on hydrogen-bonded supramolecular polymers, see: a) A. T. ten Cate, R. P. Sijbesma, *Macromol. Rapid Commun.* **2002**, *23*, 1094–1112; b) A. W. Bosman, L. Brunsveld, B. J. B. Folmer, R. P. Sijbesma, E. W. Meijer, *Macromol. Symp.* **2003**, *201*, 143–154; c) G. Armstrong, M. Buggy, *J. Mater. Sci.* **2005**, *40*, 547–559; d) P. S. Corbin, S. C. Zimmerman in *Supramolecular Polymers* (Ed.: A. Ciferri), Taylor and Francis, Boca Raton, USA, **2005**, pp. 153–185.
- [5] Recent examples of supramolecular hydrogen-bonded copolymers: a) F. Würthner, C. Thalacker, A. Sautter, W. Schärli, W. Ibach, O. Hollricher, *Chem. Eur. J.* **2000**, *6*, 3871–3886; b) V. Berl, M. Schmutz, M. J. Krische, R. G. Khoury, J.-M. Lehn, *Chem. Eur. J.* **2002**, *8*, 1227–1244; c) R. Takasawa, K. Murota, I. Yoshikawa, K. Araki, *Macromol. Rapid Commun.* **2003**, *24*, 335–339; d) F. Lortie, S. Boileau, L. Bouteiller, *Chem. Eur. J.* **2003**, *9*, 3008–3014; e) J. H. K. Ky Hirschberg, A. Ramazi, R. P. Sijbesma, E. W. Meijer, *Macromolecules* **2003**, *36*, 1429–1432; f) W. H. Binder, M. J. Kunz, E. Ingolic, *J. Polym. Sci. Part A* **2004**, *42*, 162–172; g) W. H. Binder, M. J. Kunz, C. Kluger, G. Hayn, R. Saf, *Macromolecules* **2004**, *37*, 1749–1759; h) J. Fu, E. A. Fogleman, S. L. Craig, *Macromolecules* **2004**, *37*, 1863–1870; i) G. B. W. L. Ligthart, H. Ohkawa, R. P. Sijbesma, E. W. Meijer, *J. Am. Chem. Soc.* **2005**, *127*, 810–811; j) W. H. Binder, S. Bernstorff, C. Kluger, L. Petraru, M. J. Kunz, *Adv. Mater.* **2005**, *17*, 2824–2828; k) H. Nakade, M. F. Ilker, B. J. Jordan, O. Uzun, N. L. LaPointe, E. B. Coughlin, V. M. Rotello, *Chem. Commun.* **2005**, 3271–3273; l) V. G. H. Lafitte, A. E. Aliev, P. N. Horton, M. B. Hursthouse, K. Bala, P. Golding, H. C. Hailes, *J. Am. Chem. Soc.* **2006**, *128*, 6544–6545.
- [6] F. Lortie, S. Boileau, L. Bouteiller, C. Chassenieux, F. Lauprêtre, *Macromolecules* **2005**, *38*, 5283–5287.
- [7] The DOSY-technique: a) K. F. Morris, C. S. Johnson, Jr., *J. Am. Chem. Soc.* **1992**, *114*, 3139–3141; b) C. S. Johnson, Jr., *Prog. Nucl. Magn. Reson. Spectrosc.* **1999**, *34*, 203–256; c) K. F. Morris, P. Stilbs, C. S. Johnson, Jr., *Anal. Chem.* **1994**, *66*, 211–215; for applications on hydrogen-bonded systems see for instance: d) R. J. B. Folmer, R. P. Sijbesma, E. W. Meijer, *J. Am. Chem. Soc.* **2001**, *123*, 2093–2094; e) S. Arai, D. Niwa, H. Nishide, S. Takeoka, *Org. Lett.* **2007**, *9*, 17–20.
- [8] S. H. M. Söntjens, R. P. Sijbesma, M. H. P. Van Genderen, E. W. Meijer, *J. Am. Chem. Soc.* **2000**, *122*, 7487–7493; R. K. Castellano, S. L. Craig, C. Nuckolls, J. Rebek, Jr., *J. Am. Chem. Soc.* **2000**, *122*, 7876–7882.
- [9] C. A. Hunter, S. Tomas, *J. Am. Chem. Soc.* **2006**, *128*, 8975–8979.
- [10] For dynamic systems, using method 1), the dissociation at internal positions will still take place when the ends are blocked. Using method 3), the disadvantage would be that the spectrum of possible monomers, those having acceptor and donor properties, respectively, is limited, thus limiting the number of different possible supramolecular polymers available.
- [11] The two-dimensional DOSY technique, method 2), is in many cases a solution for static (generally strong) supramolecular systems, where the diffusion coefficient  $D_i$  of each species  $i$  in the first dimension can be identified by the NMR resonance spectrum in the second, providing information about the size of the aggregates.<sup>[7d,e]</sup> However, for dynamic (generally weak) supramolecular systems, both the observed diffusion coefficient and the observed NMR resonances consist of an average of the ones for all the different species (weighted by the mole-fraction of each  $i$ ), making the DOSY technique inappropriate. In contrast, if successful, for dynamic association systems studied by the corresponding one-dimensional technique, PFG NMR, association constants can be obtained: For example, the association constant for a simple 1:1 system have been estimated assuming that the diffusion constant for the host and host-guest complex can be set equal,<sup>[7f]</sup> however, a situation far from the case with dynamic supramolecular polymers.
- [12] L. Fielding, *Tetrahedron* **2000**, *56*, 6151–6170.
- [13] A. N. Veselkov, M. P. Evstigneev, D. A. Veselkov, D. B. Davies, *J. Chem. Phys.* **2001**, *115*, 2252–2266.
- [14] For examples, see: R. P. Sijbesma, F. H. Beijer, L. Brunsveld, B. J. B. Folmer, J. H. K. K. Hirschberg, R. F. M. Lange, J. K. L. Lowe, E. W. Meijer, *Science* **1997**, *278*, 1601–1604 and references [5a,b,i].
- [15] R. B. Martin, *Chem. Rev.* **1996**, *96*, 3043–3064.
- [16] a) J. L. Dimicoli, C. Helene, *J. Am. Chem. Soc.* **1973**, *95*, 1036–1044; b) K. Weller, H. Schuetz, I. Petri, *Biophys. Chem.* **1984**, *19*, 289–298; c) F. Aradi, A. Foldesi, *Magn. Reson. Chem.* **1985**, *23*, 375–378; d) F. Aradi, A. Foldesi, *Magn. Reson. Chem.* **1989**, *27*, 249–252; e) J. Kapuscinsky, M. Kimmel, *Biophys. Chem.* **1993**, *46*, 153–163; f) J.-S. Chen, J.-C. Shiao, *J. Chem. Soc. Faraday Trans.* **1994**, *90*, 429–433; g) J. Baxter, M. P. Williamson, T. H. Lilley, E. Haslam, *J. Chem. Soc. Faraday Trans.* **1996**, *92*, 231–234; h) R. W. Larsen, R. J. Sasuja, R. Hetzler, P. T. Muraoka, V. D. Andrada, D. Jameson, *Biophys. J.* **1996**, *70*, 443–452; i) D. B. Davies, D. A. Veselkov, A. N. Veselkov, *Mol. Phys.* **1999**, *97*, 439–451; j) D. B. Davies, D. A. Veselkov, V. V. Kodintsev, M. P. Evstigneev, A. N. Veselkov, *Mol. Phys.* **2000**, *98*, 1961–1971.
- [17] K. M. Sanders, *Chem. Eur. J.* **1998**, *4*, 1378–1383.
- [18] a) S. Jónsson, F. G. J. Odille, P.-O. Norrby, K. Wärnmark, *Chem. Commun.* **2005**, 549–551; b) S. Jónsson, F. G. J. Odille, P.-O. Norrby, K. Wärnmark, *Org. Biomol. Chem.*, **2006**, *4*, 1927–1948.
- [19] a) G. G. Hammes, A. C. Park, *J. Am. Chem. Soc.* **1969**, *91*, 956–961; b) G. G. Hammes, H. O. Spivey, *J. Am. Chem. Soc.* **1966**, *88*, 1621–1625.
- [20] Cyclic dimers have been assembled using this concept by Wuest. See for example: Y. Ducharme, J. D. Wuest, *J. Org. Chem.* **1988**, *53*, 5787–5789.
- [21] a) MacroModel Version 8.5 from Schrödinger Inc., F. Mohamadi, N. G. J. Richards, W. C. Guida, R. Liskamp, M. Lipton, M. C. Caulfield, G. Chang, T. Hendrickson, W. C. Still, *J. Comput. Chem.* **1990**, *11*, 440–467; b) the energy was minimized using the MM3\* force field: N. L. Allinger, Y. H. Yuh, J.-H. Lii, *J. Am. Chem. Soc.* **1989**, *111*, 8551–8566.
- [22] P. J. Flory, *Statistical Mechanics of Chain Molecules*, Wiley, New York, **1969**.
- [23] F. Garland, S. D. Christian, *J. Phys. Chem.* **1975**, *79*, 1247–1252.
- [24] D. Zhao, J. S. Moore, *Org. Biomol. Chem.* **2003**, *1*, 3471–3491.
- [25] See references [15] and [24], and references therein.
- [26] S. E. Levinson, L. R. Rabiner, M. M. Sondhi, *Bell Syst. Tech. J.* **1983**, *62*, 1035–1074.
- [27] Noting that  $\mathbf{1}_x^T \Delta_c^{-1} = c_x^{-1} \mathbf{1}_x^T$ .
- [28] Noting that  $\mathbf{c}^T \Delta_c^{-1} = \mathbf{1}^T$ .
- [29] E. Boucher, M. Simard, J. D. Wuest, *J. Org. Chem.* **1995**, *60*, 1408–1412.
- [30] ESIMS of the equilibrium mixture was attempted but failed due to the fact that at the operating conditions for ESIMS, the solution is so diluted that the equilibrium system is far from the total concentration at which the mole fraction of cyclic trimer **7** is at its maxi-

mum. This means that for the actual system on which the ESIMS is recorded, not only the total concentration of species is low, but so is the concentration of **7**.

- [31] Cyclic structures of higher association degree are also feasible according to molecular modeling. However, due to the entropic penalty cost for their formation, they are less likely compared to the cyclic trimer.
- [32] For excellent discussions about criteria for NMR-titrations, see: "Design, Synthesis, and Evaluation of an Efficacious Functional Group Dyad. Methods and Limitations in the use of NMR for Measuring Host–Guest Interactions": C. S. Wilcox in *Frontiers in Supramolecular Organic Chemistry and Photochemistry* (Eds.: H.-J. Schneider, H. Dürr), Wiley-VCH, Weinheim, **1991**, pp. 121–143 and

K. Hirose, *J. Inclusion Phenom. Macrocyclic Chem.* **2001**, *39*, 193–209.

- [33] Care must be exercised in adding more equilibria to existing ones without having strong indications that such equilibria exist as this will add more parameters to the fit since the estimate of the variance of the fit increases monotonically with the number of parameters of the fit. See: P. J. Brockwell, R. A. Davis, *Time series: Theory and Methods*, 2nd ed., Springer, New York, **1991**, p. 287.

Received: January 9, 2007

Revised: June 16, 2007

Published online: September 17, 2007